

Dear editor and reviewers,

First of all, we would like to express our sincere appreciation to your valuable feedbacks. Your comments are highly insightful and enable us to substantially improve the quality of our manuscript and OpenArray. Below are our point-by-point responses to all comments.

1 Responses to the comments of referee #1

1.1 General Comments

While the discussion paper is well structured and clearly written I am missing some parts which I outline below. In my opinion the publication as a whole does not need to be restructured or rewritten but I suggest to extent/rewrite/restructure the introduction by describing the state of the art in somewhat more detail. I wished the authors had mentioned their solution for IO and provided a discussion section to share their experiences and opinion about the pros and cons of their approach.

[Response]:

We appreciate for your helpful suggestions. First, we have restructured the introduction section and described the state of art in more details, especially by adding comparisons to similar work (Lines 71~101). Second, we provided more details of the I/O frameworks, including implementation method and future improvement plan in the discussion section (Lines 618~624). Lastly, we added several paragraphs to present our experiences and opinion about the pros and cons of our approach in the discussion section. (Lines 572~606)

Unfortunately, I did not succeed to install OpenArray on an OSX system (macOS 10.14.3, Armadillo 9.2, Boost 1.66, LLVM 7.0, gcc/g++/gfortran 8.3, openmpi 3.0).

[Response]:

Sorry to hear that. To solve the installation issue, we prepared a simple user manual for OpenArray v1.0, which is available at https://github.com/hxmhuang/OpenArray_CXX/tree/master/doc. In section 2 of the user manual, we introduced how to install OpenArray on Linux and Mac OS operating systems step by step. If you still have any question, please feel free to contact me (hxm@tsinghua.edu.cn).

1.1.1 Introduction

While the general motivation to start the OpenArray approach is made clear in this paper I am missing a more complete discussion of the state of the art. A few approaches (ATMOL, ICON DSL, STELLA) are listed but the text does not provide useful hints in how far OpenArray really goes beyond existing approaches. I am missing ATLAS (DOI: 10.1016/j.jcp.2017.07.006). I am not an expert in this field, but to me ATLAS seems to cover several design aspects, in particular operators, support for parallelism, and support for different grid types, and seems to be in these aspects similar to OpenArray. The ESCAPE project and its follow-up ESCAPE2 worked or will work in this direction. The authors cite Lawrence et al., 2018 but only as a reference for a trend towards the usage of “heterogeneous and advanced computing platforms”, even though Lawrence et al. also discuss software approaches to address these challenges, including concepts like those used by OpenArray.

[Response]:

Thanks for your nice suggestions. We rewritten the introduction part, introducing more details about the related work, including ATMOL, ICON DSL, STELLA and ATLAS. In addition, we compared OpenArray with them in detail to demonstrate the advantages and disadvantages of OpenArray in the revised manuscript. (Lines 71~101)

“Many efforts have been made to address the complexity of parallel programming for numerical simulations, such as operator overloading, source-to-source translator and domain specific language (DSL). Operator overloading supports the customized data type and provides simple operators and function interfaces to implement the model algorithm. This technique is widely used because the implementation is straightforward and easy to understand (Corliss and Griewank, 1994; Walther et al., 2003). However, it is prone to work inefficiently because overloading execution induces numerous unnecessary intermediate variables, consuming valuable memory bandwidth resources. Using a source-to-source translator offers another solution. As indicated by the name, this method converts one language, which is usually strictly constrained by self-defined rules, to another (Bae et al., 2013; Lidman et al., 2012). It requires tremendous work to develop and maintain a robust source-to-source compiler. Furthermore, DSLs can provide high-level abstraction interfaces that use mathematical notations similar to those used by domain scientists, so that they can write much more concise and more straightforward code. Some outstanding DSLs, such as ATMOL (van Engelen, 2001), ICON DSL (Torres et al., 2013), STELLA (Gysi et al., 2015) and ATLAS (Deconinck et al., 2017), are used by the numerical model community. Although they seem source-to-source technique, DSLs are newly-defined languages and produce executable programs instead of target languages. Therefore the new syntax makes it difficult for the modellers to master the DSLs. In addition, most DSLs are not yet supported by robust compilers due to their relatively short history. Most of the source-to-source translators and DSLs still do not support the rapidly evolving heterogeneous computing platforms, such as the Chinese Sunway TaihuLight supercomputer which is based on

the homegrown Sunway heterogeneous many-core processors and located at the National Supercomputing Center in Wuxi.

Other methods such as COARRAY Fortran and CPP templates provide alternative ways. Using COARRAY Fortran, a modeller has to control the reading and writing operation of each image (Mellor-Crummey et al., 2009). In a sense, one has to manipulate the images in parallel instead of writing serial code. In term of CPP templates, it is usually suitable for small code and difficult for debugging (Porkoláb et al., 2007).”

1.1.2 IO

As a model without IO is pretty useless it would have been nice to have read a few lines about how the (parallel) IO is approached. It is included in OpenArray, so why not spending one paragraph on such an important issues as well, perhaps with some graph showing the IO performance.

[Response]:

Thanks for your valuable suggestions. We added one paragraph in the discussion section to describe the current I/O interfaces, the implementing methods, and the future plan to improve the I/O performance of OpenArray. (Lines 618~624)

“Second, the data Input/Output is becoming a bottleneck of earth system models as the resolution increases rapidly. At present we encapsulate the PnetCDF library to provide simple I/O interfaces, such as load operation and store operation. A climate fast input/output (CFIO) library (Huang et.al, 2014) will be implemented into OpenArray in the next few years. The performance of CFIO is approximately 220% faster than PnetCDF because of the overlapping of I/O and computing. CFIO will be merged into the future version of OpenArray and the performance is expected to be further improved.”

1.1.3 Discussion

You are convincing in the sense that your approach is valid and takes major burden from the oceanographer who “only” wants to run and modify an ocean model. On the other hand the complexity has not magically disappeared but it is moved from GOMO (in this example) to OpenArray. When porting the whole software onto a new system the major effort now goes into OpenArray - which is fine, but it has to be done. How complex is this? How flexible is the OpenArray approach in this respect.

[Response]:

Thanks for your helpful comments. Indeed, we moved the complexity from GOMO to OpenArray. Thus, the major burden of code porting is taken away for the oceanographers. OpenArray is designed to support multiple hardware platforms

through separating hardware-dependent functions such as low-level numerical computations from the main framework.

We added a paragraph to introduce the complexity of the migration in section 3.4 (Lines 412-426): “With the help of dynamic code generation and JIT compilation technology, OpenArray can be migrated to different backend platforms. Several basic libraries, including Boost C++ libraries and Armadillo library, are required. The JIT compilation module is based on Low-Level-Virtual-Machine (LLVM), thus theoretically the module can only be ported to platforms supporting LLVM. If LLVM is not supported, as on the Sunway platform, one can generate the fusion kernels in advance by running the ocean model on an X86 platform. If the target platform is CPUs with acceleration cards, such as GPU clusters, it is necessary to add control statements in the CPU code, including data transmission, calculation, synchronous and asynchronous statements. In addition, the accelerating solution should involve the selection of the best parameters, for example “blockDim” and “gridDim” on GPU platforms. In short, the code generation module of OpenArray also needs to be refactored to be able to generate codes for different backend platforms. The application based on OpenArray can then be migrated seamlessly to the target platform. Currently, we have designed the corresponding source code generation module for Intel CPU and Sunway processors in OpenArray.”

If the unlucky oceanographer comes up with the idea to try out yet another (perhaps higher-order) advection or any other scheme which is not yet supported by OpenArray, how difficult is it to extend OpenArray? Does this require expert knowledge and support from OpenArray developers? How seamless is - in your opinion - the integration of other stencils into the OpenArray library? I am not insisting on answering these questions line by line but rather take these as suggestions for what could be addressed in a thorough discussion. You as authors may wish to stress different - and in your opinion more important - points.

[Response]:

Thanks for your comments. We answered your questions about customized stencil operators in the discussion section. (Lines 599~606)

“The second issue is that the current OpenArray version cannot support customized operators. When modellers try out another higher-order advection or any other numerical scheme, the twelve basic operators provided by OpenArray are not abundant. We consider using a template mechanism to support the customized operators. The rules of operations are defined in a template file, where the calculation form of each customized operator is described by a regular expression. If users want to add a customized operator, they only need to append a regular expression into the template file.”

1.2 Specific Comments

Line 39 and elsewhere: consider to replace “climate model” by “Earth system model”, as the latter is now mainly used when talking about multi-component models in the context of Earth system and climate modelling efforts.

[Response]:

Thanks for the suggestion. In the revised manuscript, we have replaced “climate model” by “earth system model” in Line 35, 43, 58, 60, and 64.

Line 41: Please rephrase the sentence, as computing platforms are not applied but used.

[Response]:

Corrected. We have replaced “applied” with “used” in the sentence. (Line 46)

Line 55: Which gap do you precisely have in mind? Do you really mean climate science in general or rather climate modelling (aka Earth system modelling)?

[Response]:

Sorry for the confusion. The gap refers to a big obstacle between scientific inspiration and code implementation in the climate modeling community.

Therefore, we changed the sentence “... create a very large gap in climate science” with “...create a very large gap between scientific aspiration and code implementation in the climate modeling community”. (Lines 60~62)

Line 70: What is the former, what is the latter language? Could you briefly explain to the non-experts amongst the readers the difference between source-to-source and DSL? Perhaps this whole paragraph needs some restructuring (see remarks in my section 1.1).

[Response]:

Thanks for your comments. In the sentence, the former and the latter stand for one language and another. As indicated by the name, source-to-source method converts one language, which is usually strictly constrained by self-defined rules, to another. DSLs are newly-defined languages and produce executable programs instead of target languages. As described in the section 1.1.1, we rewritten the paragraph to give a clear description (Lines 71~95).

Line 90: Please introduce the reader to the heterogeneity you have in mind here. What makes TaihuLight different in terms of heterogeneity? From the system specification further down in your text, TaihuLight does not look that heterogeneous.

[Response]:

Sorry for the confusion. Heterogeneity refers to systems deploying multiple types of processing elements within a single workflow, and allowing each to perform the tasks to which it is best suited (Shan Amar, 2006). The major innovation of the Sunway TaihuLight supercomputer is the homegrown Sunway many-core processor which consists of 4 core-groups. Each core-group includes 64 computing processing elements

(CPEs) and a management processing element (MPE) (Fig. 1). CPE and MPE are different processing elements, the CPEs perform large-scale computing tasks and MPE are responsible for the task scheduling and communication. “The MPE is like a CPU core, and the CPE cluster is like a many-core accelerator, both the CPU and accelerator are now fused into one Sunway processor with a unified memory space” (Haohuan Fu et al, 2016, <https://link.springer.com/article/10.1007/s11432-016-5588-7>). The MPE-CPE hybrid architecture of Sunway TaihuLight makes Sunway TaihuLight heterogeneous and powerful.

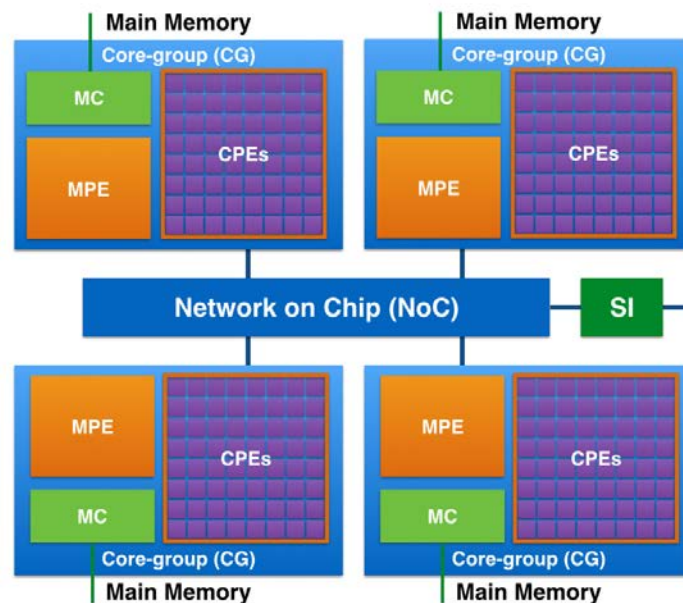


Figure 1. The MPE-CPE hybrid architecture of the Sunway processor. Every Sunway processor includes 4 Core-groups (CGs) connected by the Network on Chip (NoC). Each CG consists of a management processing element (MPE), 64 computing processing elements (CPEs) and a memory controller (MC). The Sunway processor uses the system interface (SI) to connect with outside devices.

To make a clear description, we added the following sentences in the revised manuscript.

“Over the next few decades, tremendous computing capacities will be accompanied by more heterogeneous architectures which are equipped with two or more kinds of cores or processing elements (Shan, 2006), ...” (Lines 54~56)

“..., such as the Chinese Sunway TaihuLight supercomputer which is based on the homegrown Sunway heterogeneous many-core processors and located at the National Supercomputing Center in Wuxi.” (Lines 93~95)

“According to the TOP500 list released in November 2018, the Sunway TaihuLight is ranked third in the world, with a LINPACK benchmark rating of 93 Petaflops provided

by Sunway many-core processors (or Sunway CPUs). As shown in Fig. 9, every Sunway CPU includes 260 processing elements (or cores) that are divided into 4 core-groups. Each core-group consists of 64 computing processing elements (CPEs) and a management processing element (MPE) (Qiao et al., 2017). CPEs handle large-scale computing tasks and MPE is responsible for the task scheduling and communication. The relationship between MPE and CPE is like that between CPU and many-core accelerator, except for they are fused into a single Sunway processor sharing a unified memory space.” (Lines 428~437)

Line 100: I would say that you solved the problem for one ocean model or a particular class of ocean models but not yet for ocean models in general.

[Response]:

Thanks for your corrections. We have added “a particular class of” in front of “ocean models using the finite difference method and staggered grid in OpenArray.” (Line 110)

Line 109: Is it really valid Fortran code, or shouldn't it better be classified as pseudo Fortran code as GOMO cannot really live without the OpenArray library?

[Response]:

Sorry for the confusion. OpenArray works as an independent library and it is the essential component of GOMO, since GOMO uses the functions and modules provided by OpenArray, such as average operators, differential operators, assignment functions, I/O functions, et al. Whereas, GOMO is written by valid Fortran codes.

Line 111: Is it really meant like that you compile and link one executable which can then be executed on any computing platform? Or are you talking about the intermediate C++ code? But this would require compiling and linking on the target system before it can be executed.

[Response]:

Sorry for the confusion. We transfer the cross-platform complexity to OpenArray. When porting the ocean models to a new platform, we need to redesign an additional function for the target system and add it to the code generation module in OpenArray. This added function is used to translate the intermediate computation graph into corresponding executable code for the target platform. At present, OpenArray supports X86 and Sunway platforms, therefore GOMO is executable on the two platforms without additional modification.

We rewritten the sentences (Lines 117~121): “Currently OpenArray supports both CPU and Sunway platforms. More platforms including GPU will be supported in the future. The complexity of cross-platform migration is moved from the models to OpenArray. The applications based on OpenArray can then be migrated seamlessly to the supported platform.”

Line 120: True but only if the OpenArray has been ported to and is available on the Sunway platform. There is probably no free lunch when moving to a new hardware or software environment.

[Response]:

Agree. If we want to move GOMO to a new hardware or software environment, we should make OpenArray available on the new hardware platform since OpenArray is the footstone of GOMO. In fact, we transfer the burden of porting code from application to developing library, thus decoupling the ocean models from the hardware platforms is possible.

Therefore, we added the sentences to stress that (Lines 118~121): “The complexity of cross-platform migration is moved from the models to OpenArray. The applications based on OpenArray can then be migrated seamlessly to the supported platform.”

Line 148 and elsewhere: Equation 1 is probably taken from the POM user manual, but nevertheless should not expressions like $\frac{\partial DU}{\partial x}$ rather be written as $\frac{\partial}{\partial x}(DU)$?

[Response]:

Thanks for your suggestions. Indeed, the Eq. 1 is derived from the POM user manual. Therefore, we would like to use the same expressions of the equations with that in POM user manual (shown as the following equation). This form is helpful to remove numbers of parentheses in Appendix A: Continuous governing equations.

$$\frac{\partial DU}{\partial x} + \frac{\partial DV}{\partial y} + \frac{\partial \omega}{\partial \sigma} + \frac{\partial \eta}{\partial t} = 0$$

Line 152: Could provide some hint on how to arrive at the discrete expression (2).

[Response]:

Thanks for your suggestions. We added the following details of Arakawa C grid and finite difference method to demonstrate the process from Eq. (1) to the discrete Eq. (2). (Lines 161~172)

“In Arakawa C grid, D is calculated at the centers, U component is calculated at the left and right side of the variable D , V component is calculated at the lower and upper side of the variable D (Fig. 1). Variables (D , U , V) located at different positions own different sets of grid increments. Taking the term $\frac{\partial DU}{\partial x}$ as an example, we firstly apply linear interpolation to obtain the D 's value at U point represented by $tmpD$. Through a backward difference to the product of $tmpD$ and U , then the discrete expression of $\frac{\partial DU}{\partial x}$ can be obtained.

$$tmpD(i+1,j) = 0.5*(D(i+1,j)+D(i,j)), \tag{2}$$

and

$$\frac{\partial DU}{\partial x} = \frac{tmpD(i+1,j)-tmpD(i,j)}{dx(i,j)^*} = \frac{0.5*(D(i+1,j)+D(i,j))*U(i+1,j)-0.5*(D(i,j)+D(i-1,j))*U(i,j)}{dx(i,j)^*}, \quad (3)$$

where $dx(i,j)^*=0.5*(dx(i,j) + dx(i-1,j))$.

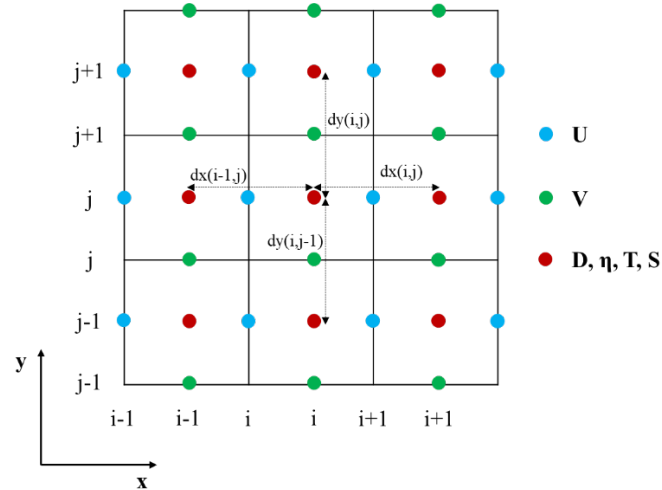


Figure 2. Arrangement of variables in the staggered Arakawa C grid. (Numbered as ‘Figure 1’ in the revised manuscript)

Line 211: I thought your current implementation of the operators only supports uniform (=equidistant) grids? What am I missing here?

[Response]:

Sorry for the confusion. In OpenArray, grid increments (dx , dy , dz) are combined with physical variables through grid binding. On the staggering Arakawa C-grid, the components of velocity (u , v , w) and potential temperature (T) et al are defined at different points. Variables on each point has its own set of grid increments so the current implementation of the operators supports varying grids.

We have changed the sentence “..., the operators can automatically set the correct grid increments for different Array variables.” into “..., a set of grid increments, including horizontal increments ($dx(i,j)$, $dy(i,j)$) and vertical increment ($dz(k)$), will be combined with each corresponding physical variable through grid binding. Thus, the operators can implicitly set the correct grid increments for different Array variables, even if the grid is nonuniform.” (Line 236~240)

Line 214 and elsewhere: I suggest to avoid the phrase “automatic”. Nothing is done automatically but every effect has a cause. Here, something is happening because you programmed it that way and some conditions are coming together to trigger an action.

[Response]:

Thanks for your corrections. We have replaced all the phrases “automatic/automatically” with “implicit/implicitly” in the revised manuscript. A programmer that writes implicitly parallel code does not need to worry about task division or process

communication, focusing instead on the problem that his or her program is intended to solve.[From wikipedia: Implicit parallelism]

Line 238: Could you clarify how the Arakawa grid type, the jumping rules and the differential operators are linked together? Let us assume I have formulated my ocean model on an Arakawa C grid and now for curiosity would like to run it on an A grid (not because it would really makes sense but to demonstrate the effect of discretization on the numerical solution) what would I have to change in my ocean model code?

[Response]:

Thanks for your valuable suggestion. To make it clearer, we took the Eq. (1) switching from Arakawa C grid to Arakawa B grid as an example, to illustrate the modifications to the ocean models when grid scheme is changed in the revised manuscript. (Lines 264~274)

“If users change the Arakawa grid type, first the position information of each physical variable need to be reset (Shown in Fig. 4). Then the discrete form of each equation needs to be redesigned. We take the Eq. (1) switching from Arakawa C grid to Arakawa B grid as an example. The positions of the horizontal velocity Array U and Array V are changed to Point 0, Array η and Array D stay the same. The discrete form is changed from Eq. (4) to Eq. (13), the corresponding implementation by operators is changed from Eq. (6) to Eq. (14).”

$$\frac{\eta_{t+1}(i,j)-\eta_{t-1}(i,j)}{2*dt} + \frac{0.25*(D(i+1,j)+D(i,j))*(U(i+1,j)+U(i+1,j+1))-0.25*(D(i,j)+D(i-1,j))*(U(i,j)+U(i,j+1))}{dx(i,j)*} + \frac{0.25*(D(i,j+1)+D(i,j))*(V(i,j+1)+V(i+1,j+1))-0.25*(D(i,j)+D(i,j-1))*(V(i,j)+V(i+1,j))}{dy(i,j)*} = 0 \quad (13)$$

$$\eta_{t+1} = \eta_{t-1} - 2 * dt * \left(\delta_f^x \left(\bar{D}_b^x * \bar{U}_f^y \right) + \delta_f^y \left(\bar{D}_b^y * \bar{V}_f^x \right) \right) \quad (14)$$

Line 247: What is the motivation for the list of ocean model codes you provide in this paragraph? There are other codes around, e.g. FESOM (see <https://fesom.de> and the list of publication there) or an unstructured grid model for global ocean dynamics by P. Korn (see <https://doi.org/10.1016/j.jcp.2017.03.009>) and several more.

[Response]:

Sorry for the confusion. In this paragraph, we want to express our respect to these excellent ocean models, such as POM, ROMS, MITgcm, and FESOM. From these models, we obtained abundant experience and knowledge leading us to build OpenArray. Considering most of these existing ocean models using finite difference or finite volume methods on structured meshes, we designed 12 basic operators in OpenArray only for this particular class of ocean models at present. In our future work, more customized operators will be implemented to support other numerical methods and meshes.

We simplified the paragraph (Lines 284~291): “Although most of the existing ocean models use finite difference or finite volume methods on structured or semi-structured meshes (e.g., Blumberg and Mellor, 1987; Shchepetkin and McWilliams, 2005), there are still some ocean models using unstructured meshes (e.g., Chen et al., 2003; Korn, 2017), and even the spectral element method (e.g., Levin et al., 2000). In our current work, we design the basic operator only for finite difference and finite volume methods with structured grids. More customized operators for the other numerical methods and meshes will be implemented in our future work.”

Line 274 section 3.1: Could you add a few lines to describe the handling of lateral and vertical boundary conditions within your operators?

[Response]:

Thanks for your comments. In section 3.3, we added the details to describe how to handle the lateral and vertical boundary conditions within the operators (Lines 406~409): “For the global boundary conditions of the limited physical domains, the values at the physical border are always set to zero within the operators and operator expressions. In realistic cases, the global boundary conditions are set by a series of functions (e.g., radiation, wall) provided by OpenArray.”

Line 334: When speaking of subgraphs and the kernel function, can the individual advection and diffusion terms be accessed for diagnostic purposes?

[Response]:

Thanks for your comments. If users want access to individual variables or subgraphs, they need to split the formula or code into multiple expressions for diagnostic or printing purposes.

We added the sentence to introduce the access to any subgraphs (Lines 367~369): “Users can access to any individual subgraph by assigning the subgraph to an intermediate variable for diagnostic purposes.”

Line 352: I am not sure what is meant here and perhaps the sentence should be rephrased. Such a function needs to be programmed once for a particular ocean model, but once it is there it can be used, see e.g. ESMF_FieldBundleHalo contained in the Earth System Modeling Framework (ESMF). To my knowledge, other ocean models use similar approaches for the halo exchange as well. But no doubt, it is a relief to have it.

[Response]:

Thanks for your suggestions. Earth system models generally provide simple functions (e.g. ESMF_FieldBundleHalo) for users to manually control the communication of boundary regions. In OpenArray, we further hide these communication through the fused kernel. Users do not need to care about the halo exchange, or know the parallel details.

The sentence has been rephrased (Lines 396~397): “Clearly, ocean modellers have to frequently call corresponding functions to carefully control the communication of the local boundary region.”

Line 391: Is the mode splitting algorithm inherited from POM, if so, this should be mentioned.

[Response]:

Thanks for your suggestion. Indeed, the mode splitting algorithm is inherited from POM. Therefore, we have changed “... the mode-splitting algorithm to address ...” into “... the mode-splitting algorithm inherited from POM to address ...” (Lines 454~455)

Line 422: Could you provide the number of lines for OpenArray as well? I could calculate it myself but . . .

[Response]:

Thanks for your suggestion. The code of OpenArray is about 11,800 lines. We added the sentences to provide the number of lines for OpenArray. (Lines 493~495): “since the complexity has been transferred to OpenArray, which includes about 11,800 lines of codes.”

Line 425: You raise the impression that porting is not an issue anymore. While this is certainly true for GOMO (which is of course very valuable) the porting still has to be done for OpenArray. Maybe this could be clarified somewhere (perhaps in the discussion).

[Response]:

Thanks for your comments. Indeed, since the porting has been transferred to OpenArray, the models can be run on these platforms supported by OpenArray.

Therefore, we added the clarification in our revised manuscript. (Lines 118~121): “The complexity of cross-platform migration is moved from the models to OpenArray. The applications based on OpenArray can then be migrated seamlessly to the supported platform.”

Line 469 section 5.3: Which hardware do you use for these tests? What sets the upper bound of 4096 processes?

[Response]:

Thanks for your comments. In section 5.3, the strong and weak scaling experiments were taken on the X86 cluster at National Supercomputing Center in Wuxi of China, which provides 5000 Intel Xeon E5-2650 v2 CPUs for our account at most. In the future, we will increase the upper bound if more computing resources are available.

We added the sentences to provide more details (Lines 543~545): “We use the X86 cluster at National Supercomputing Center in Wuxi of China, which provides 5000 Intel Xeon E5-2650 v2 CPUs for our account at most.”

Line 481 section 5.4: What does this mean for a reasonable local domain size? 32X32 points as in sec. 5.3 is still on the good side, while 9x9 as used on TaihuLight does shows some performance degradation.

[Response]:

Thanks for your comments. On the same machine architecture, the parallel efficiency is usually better if the local domain size is bigger. The weak and strong scaling experiments in section 5.3 were taken on X86 cluster, while the experiment in section 5.4 was taken on the Sunway processors. As described above, the architecture of Sunway platform is largely different from X86 machine.

We added the sentences in section 5.3 to make a clear description (Lines 543~545): “We use the X86 cluster at National Supercomputing Center in Wuxi of China, which provides 5000 Intel Xeon E5-2650 v2 CPUs for our account at most.”

In section 5.4, we changed the sentence “The strong scalability of GOMO is also tested on the Sunway TaihuLight supercomputer.” into “We also test the scalability of GOMO on the Sunway platform.” (Line 555)

Line 490: As I understand the steps up to compiling the JIT are done only once at the beginning of a job. If you run a longer experiment (in terms of wallclock time or number of timesteps) the initialisation phase should be negligible when compared to the total run time. Why don't you provide two numbers, one for the initialisation and one for the integration within the time loop?

[Response]:

Agree. The fusion-kernel codes are generated and compiled only once at the beginning of a job. In the scalability tests of GOMO, this initialization phase consumes about 2 minutes.

We added the sentence to introduce the time consumption (Lines 564~566): “Even though the fusion-kernel codes are generated and compiled only once at the beginning of a job, it consumes about 2 minutes.”

1.3 Technical Corrections/Suggestions

L39 climate model → climate models

[Response]:

We changed the “climate model” into “earth system models”. (Line 43)

L42 climate community → climate modelling community

[Response]:

Corrected.

L43 model program needs → model programs need

[Response]:

Corrected.

L68 inefficiency → inefficiently

[Response]:

Corrected.

L83 the sentence needs to be reordered. It is not clear (to me) to which part “at the product level” is referring to.

[Response]:

Sorry for the confusion. We rewritten the whole paragraph. To make a clear description, the sentence has been replaced with “It requires tremendous work to develop and maintain a robust source-to-source compiler.” (Lines 81~82)

L106 change to : . . . is similar to the original but manually optimized parallel program.

[Response]:

Corrected.

L108 support → supports

[Response]:

Corrected.

L125 → The implementation

[Response]:

Corrected.

L139 → In traditional ocean models . . .

[Response]:

Corrected.

L143 → When using the OpenArray library . . .

[Response]:

Corrected.

L211 → we propose

[Response]:

Corrected.

L220 → . . . the horizontal velocity components $\text{Array}(U)$ and $\text{Array}(V)$ are . . . or
. . . the horizontal velocity $\text{Array}(U, V)$ is . . .

[Response]:

Thanks for your corrections. We have changed the sentence “. . . the horizontal velocity $\text{Array}(U, V)$ are . . .” into “. . . the horizontal velocity *Array* (U, V) is . . .” (Line 246)

L238 can be used → are used

[Response]:

Corrected.

L257 different → difference; operator → operators

[Response]:

Corrected.

L289 will be concealed by → is hidden behind

[Response]:

Corrected. We changed “will be concealed by” into “are hidden behind”.

L290 → : : : and can escape . . .

[Response]:

Corrected.

L303 → to implement a so-called lazy expression . . .

[Response]:

Corrected.

L318 . . .AYF are the interpolated functions → . . .AYF are the average functions.

[Response]:

Corrected.

L373 computing processing elements: aren't these Central Processing Units (CPUs)

[Response]:

Sorry for the confusion. The computing power of TaihuLight is provided by a homegrown Sunway many-core processor (or Sunway CPU). The Sunway CPU includes four core-groups (CGs). Each CG includes one management processing element (MPE), 64 computing processing elements (CPEs), and one memory controller (MC). CPEs can only perform computations and MPE are responsible for the task scheduling and communication. Traditionally, the term "CPU" refers to a processor, including processing unit and control unit at least. Therefore, computing processing elements are not regarded as CPUs.

Therefore, we added more details of computing processing elements in section 3.4 (Lines 433~437): “CPEs handle large-scale computing tasks and MPE is responsible for the task scheduling and communication. The relationship between MPE and CPE is like that between CPU and many-core accelerator, except for they are fused into a single Sunway processor sharing a unified memory space.”

L384 a practical ocean model → a numerical ocean model

[Response]:

Corrected.

L404 rephrase, the TKE and alike can be calculated but not the submodel.

[Response]:

Thanks for the suggestion. We have changed the sentence “..., and turbulence closure sub-model (q2, q2l) (Mellor and Yamada, 1982)” into “..., and turbulence closure scheme (q2, q2l) (Mellor and Yamada, 1982)”.

L505 a practical ocean model → a numerical ocean model

[Response]:

Corrected.

2 Responses to the comments of David Webb

Thanks for your valuable feedbacks again. Your comments for the OpenArray and my previous article (POM.gpu) are always highly insightful and enable us to improve the quality of our manuscripts. Below are our point-by-point responses to all your comments and our plans to revise the manuscript.

1. “This is a well written paper concerned with generating an ocean model from a set of equations closer in form to the underlying differential equations than is usual. It is an interesting computational exercise but the resulting code has some important deficiencies and for that reason I think it would be more suited for a computational journal than the present one.”

[Response]:

We are very happy to hear that you are satisfied with our paper written. Although it looks like a general computing tool, OpenArray is particularly designed for earth system models. It is a product of collaboration between oceanographers and computer scientists. We aim to promote it to the model community as a development tool for the future numerical models. We believe it is of great help for the development of ocean models and we sincerely hope it to be widely used by ocean modellers. That is why we submit our manuscript to GMD to advertise our work.

We have modified the abstract (Lines 23~26) to stress its significance for the model development, extended the introduction (Lines 71~101) to compare with existing studies, and added a new discussion section (Lines 572~635) to describe the pros and cons of OpenArray.

2. “My main concerns all involve computational efficiency. As the authors state, ocean models are memory bandwidth limited and for that reason the code is usually written in such a way that once a variable is in one of the processor registers or in the highest speed cache it is used as much as possible before being replaced. In fact the aim should be never to move variables more than once each timestep. In the present code the authors spend a major section reporting on one small step in this direction, but really this should only be the first of many steps.”

[Response]:

Totally agree, computational efficiency is a big challenge. We have to admit we cannot fully solve the memory bandwidth limited problem at the current stage, but the main purpose of OpenArray is to provide a user-friendly, platform-independent tool for the development of ocean models. The memory consumption by similar techniques such as operator overloading is much higher due to the unnecessary intermediate variables. In contrast, the memory consumption by OpenArray is significantly reduced to a level similar to the ocean models developed in the conventional way. In OpenArray, we adopted a series of optimization methods to alleviate the requirement of memory

bandwidth. We will further make continuous efforts to optimize the performance of OpenArray in the future version, using the techniques including time skewing and polyhedral model. Therefore, we added the following paragraphs to discuss the memory bandwidth limitation. (Lines 583~597)

“However, there are still several problems to be solved in the development of OpenArray. The first issue is computational efficiency. Once a variable is in one of the processor registers or in the highest speed cache, it should be used as much as possible before being replaced. In fact, we should never to move variables more than once each timestep. The memory consumption brought by overloading techniques is usually high due to the unnecessary variable moving and unavoidable cache missing. The current efficiency and scalability of GOMO are close to sbPOM, since we have adopted a series of optimization methods, such as memory pool, graph computing, JIT compilation, and vectorization, to alleviate the requirement of memory bandwidth. However, we have to admit that we cannot fully solve the memory bandwidth limited problem at present. We think that time skewing is a cache oblivious algorithm for stencil computations (Frigo and Strumpen, 2005), since it can exploit temporal locality optimally throughout the entire memory hierarchy. In addition, the polyhedral model may be another potential approach, which uses an abstract mathematical representation based on integer polyhedral, to analyze and optimize the memory access pattern of a program.”

3. “I am also concerned about the way the code deals with multi-processor architectures. Unfortunately, although I was able to compile both the c++ and fortran sections, the link step failed and so I was not able to check the running code. However the main time stepping loop appears to run on a single processor and it is only the difference and averaging operators, in the c++ code, which make use of the multi-processor architecture. This is surprising given the authors emphasis on the importance of parallel computing.”

[Response]:

We are so sorry for the failure in the link step. The other referee also reported this bug. We have fixed this bug and we submitted a simple user manual including installation instructions, description of functions, application examples and debug methods, etc. on the GitHub (https://github.com/hxmhuang/OpenArray_CXX/tree/master/doc).

We emphasis on the importance of parallel computing because the operators in OpenArray, not only the difference and average operators, but also the “+”, “-”, “*”, “/” and “=” operators in the Fortran code, are all implicit parallelism. It is the most prominent feature of the program using OpenArray.

Therefore, we added a paragraph in Section 4 to describe more details (Lines 473~479): “When the user dives into the GOMO code, the main time stepping loop in GOMO appears to run on a single processor. In fact, implicit parallelism is the most prominent feature of the program using OpenArray. The operators in OpenArray, not only the

difference and average operators, but also the “+”, “-”, “*”, “/” and “=” operators in the Fortran code, are all overloaded for the special data structure “Array”. The seemingly serial Fortran code is implicitly converted to parallel C++ code by OpenArray, and the parallelization is hidden from the modellers.”

4. “I am also a bit wary about all the details being lost in the c++ compiler/interpreter code. The authors emphasize the possibility of portability but this implies a large organization continually keeping such a code up to date and adapted to the latest hardware. If not, the climate modelling groups have to do it themselves in which case the effort required will be much the same as now except for the addition of the compiler/interpreter and associated packages.”

[Response]:

Thanks for your valuable suggestions. Indeed, we aim to develop OpenArray into a stable and community software, just like the C/C++/Fortran compiler or math library. We will follow the GNU open source license. In general, the programmers do not need to worry about the technical details of a compiler too much, especially for the oceanographers. Our original intention was to provide simple Fortran interfaces and the C++ section is totally hidden by OpenArray. In addition, the developing team of OpenArray consists of researchers from the National Supercomputing Center in Wuxi and Tsinghua University. OpenArray will be an important software to simplify the porting work on the Sunway TaihuLight supercomputer. The Sunway TaihuLight supercomputer has been the world's fastest supercomputer for two years, from June 2016 to June 2018, according to the TOP500 lists. The OpenArray project is supported by some long-term grants. Therefore, the project will be stably maintained for at least 4 years.

We added some sentences in the section 3.3 to introduce how the subgraphs are converted into C++ code (Lines 374~379): “In order to generate a kernel function based on a subgraph, we firstly add the function header and variable definitions according to the name and type in the *Array* structure. And then we add the loop head through the dimension information. Finally, we perform a depth-first walk on the expression tree to convert data, operator, and assignment nodes into a complete expression including load variables, arithmetic operation, and equal symbol with C++ language.”

In addition, we added the following paragraph to stress the aim of OpenArray and its role in model development (Line 631~635): “OpenArray is a product of collaboration between oceanographers and computer scientists. It plays an important role to simplify the porting work on the Sunway TaihuLight supercomputer. We believe that OpenArray and GOMO will continue to be maintained and upgraded. We aim to promote it to the model community as a development tool for the future numerical models.”

5. “Both of the architectures discussed appear to be cache based but as I understand it the next major advance will come from better use of gpus. In these systems I expect

variables will stay in gpu memory or be swapped between gpus and rarely return to the main cpu memory. For such systems the structure proposed here appears unsuitable.”

[Response]:

Thanks for your helpful comments. In addition to CPU platform, the current version of OpenArray supports the Sunway TaihuLight supercomputer which represents the major advance in China, since we are affiliated to the National Supercomputing Center in Wuxi. As you know, most of the current ocean models are still running on the CPU architecture. Our plan is to develop stable and efficient OpenArray on the both discussed architectures first, and then migrate it to GPU. Actually, the GPU version of OpenArray is already under development.

We introduced the details of GPU version of OpenArray in the discussion section. (Lines 611~616): “First, we are developing the GPU version of OpenArray. During the development, the principle is to keep hot data staying in GPU memory or directly swapping between GPUs and avoid returning data to the main CPU memory. NVLink provides high bandwidth and outstanding scalability for GPU-to-CPU or GPU-to-GPU communication, and addresses the interconnect issue for multi-GPU and multi-GPU/CPU systems.”

6. “There is also the question of how researchers might try out new code with the prosed library and debug the resulting runs. No user manual is provided and it is difficult to see how bugs can be traced, especially if they involve the c++ section of the code.”

[Response]:

A user manual and several application examples have been released on GitHub to help users to install and use OpenArray, a reference manual including more details is currently under preparation. In addition, we have added several functions for debugging (shown in Tab. 1) and these functions are proved very useful during the ocean model (GOMO) development. In the future, more debugging functions will be implemented to trace and solve the potential bugs.

Table 1. Functions for debugging in OpenArray

Functions	Description
display()	print the value of an array
display_array_info()	print the information of an array
save()	save an array to a given file
sum()	sum array in a given direction
csum()	cumulative sum an array in a given direction
max()	get the maximum value of an array
min()	get the minimum value of an array
max_at()	get the position of the maximum value
min_at()	get the position of the minimum value

We added a sentence in the Code availability section (Lines 654~655): "... and the user manual of OpenArray can be accessed at https://github.com/hxmhuang/OpenArray_CXX/tree/master/doc".

7. "I also do not understand why a just-in-time compiler is used, given that the model grids do not change in time so that both human and computer effort would be better spent optimizing the fixed grid code. And on this theme I am also concerned, although I would like to be proved wrong, that what has been achieved here is little different from what might be achieved with a good fortran coarray code, together with statement functions or cpp define statements to take the place of the operators."

[Response]:

Thanks for your helpful comments. The just-in-time compiler used in OpenArray can fuse numbers of operators into a large compiled kernel. The benefit of fusing operators is to reduce memory bandwidth requirements and improve performance compared to executing operators one-at-a-time. Comparing with COARRAY Fortran, OpenArray supports implicit parallelism so that a modeller does not need to worry about task division or process communication. Using COARRAY Fortran, a modeller has to control the reading and writing operation of each image. In a sense, one has to manipulate the images in parallel instead of writing serial code. In term of CPP templates, it is usually suitable for small code and difficult for debugging.

Therefore, we added the sentences to explain why we used the JIT compiler (Lines 371~374): "The JIT compiler used in OpenArray can fuse numbers of operators into a large compiled kernel. The benefit of fusing operators is to alleviate memory bandwidth limitations and improve performance compared with executing operators one-by-one."

In addition, we added the difference between OpenArray and COARRAY Fortran/CPP templates (Lines 97~101): "Other methods such as COARRAY Fortran and CPP templates provide alternative ways. Using COARRAY Fortran, a modeller has to control the reading and writing operation of each image (Mellor-Crummey et al., 2009). In a sense, one has to manipulate the images in parallel instead of writing serial code. In term of CPP templates, it is usually suitable for small code and difficult for debugging (Porkoláb et al., 2007)."

8. "One reason that these are not used in ocean models comes from the fact that in a typical ocean model only about half the theoretical 3-D grid is involved in the calculation, the rest representing land or ocean topography. When computer memory and power is readily available a factor of two does not really matter but given the computational cost of many ocean models, spending time on such cells, as usually happens when coarrays are used, can be critical."

[Response]:

Thanks for your valuable comments. Indeed, the load imbalance is one of the major issues about computational efficiency of ocean models. The land points accounting for over 30 percent are needed to be masked in the ocean grid. It is a common problem in

most of the existing ocean models. We will adopt the space-filling curve and curvilinear orthogonal grid method to solve this issue in our future version.

Therefore, we added a paragraph in discussion section to emphasize this computational problem and provide several possible solutions (Lines 626~629): “Finally, as most of the ocean models, GOMO also faces the load imbalance issue. We are adding the more effective load balance schemes, including space-filling curve (Dennis, 2007) and curvilinear orthogonal grids, into OpenArray in order to reduce the computational cost on land points.”

9. “Anyway - you can see that I am unhappy. However I must emphasise that I can also see that the paper represents a lot of hard work and I accept that as an example of an attempt to tackle good computational problem it is worthwhile. For this reason I think that publication in a journal more closely linked to the development of artificial intelligence would be more suitable.”

[Response]:

We sincerely appreciate your affirmation of our work. In fact, OpenArray is based on the joint efforts of climate modeling and high-performance computing scientists. We aim to promote it to the model community as a development tool for the future numerical models. Thus we think this work fits the aim and scope of GMD well.

We added the following sentences to introduce the role of OpenArray in model development (Lines 631~635): “OpenArray is a product of collaboration between oceanographers and computer scientists., we aim to promote it to the model community as a development tool for the future numerical models.”

10. “If on the basis of the other referees reports, the authors are asked to provide a revised version then there are two extra documents I would like to see in the additional documentation section. The first is a user manual. The second is a full list of the include files and libraries needed (i.e. all those which are not the fortran or c++ compiler files) - to help with the problems I had.”

[Response]:

Thank you for the opportunity. We have finished a simple user manual. In the installation section, we listed all pre-installed software and libraries required by OpenArray. The user manual is available on GitHub now (https://github.com/hxmhuang/OpenArray_CXX/tree/master/doc).

We really appreciate your highly constructive comments. We hope you will be satisfied with the above reply. If there are any questions, please contact us for free.

Best wishes,

Xiaomeng Huang, Xing Huang, Dong Wang, and Yi Li.

1 **OpenArray v1.0: A Simple Operator Library for the Decoupling of**

2 **Ocean Modelling and Parallel Computing**

3
4 Xiaomeng Huang^{1,2,3}, Xing Huang^{1,3}, Dong Wang^{1,3}, Qi Wu¹, Yi Li³, Shixun Zhang³,
5 Yuwen Chen¹, Mingqing Wang^{1,3}, ~~Yi Li³~~, Yuan Gao¹, Qiang Tang¹, Yue Chen¹, Zheng
6 Fang¹, Zhenya Song^{2,4}, Guangwen Yang^{1,3}

7
8 ¹ Ministry of Education Key Laboratory for Earth System Modeling, Department of
9 Earth System Science, Tsinghua University, Beijing 100084, China

10 ² Laboratory for Regional Oceanography and Numerical Modeling, Qingdao National
11 Laboratory for Marine Science and Technology, Qingdao, 266237, China

12 ³ National Supercomputing Center in Wuxi, Wuxi, 214011, China

13 ⁴ First Institute of Oceanography, Ministry of Natural Resources, Qingdao, 266061,
14 China

15
16 Corresponding author: hxm@tsinghua.edu.cn

17 **Abstract**

18 ~~TheThe increasing complexity of climate models combined with~~ rapidly evolving
19 computational techniques are makingintroduces a large gap between scientific
20 aspiration and code implementation in climate modelling. In this work, we design a
21 simple computing library to bridge the gap and decouple the work of ocean modelling
22 from ~~the work of~~ parallel computing. ~~ThisThe~~ library provides twelve basic operators
23 that feature user-friendly interfaces, effective programming and implicit parallelism.
24 Several state-of-art computing techniques, including computing graph and Just-In-Time
25 compiling are employed to parallelize the seemingly serial code and speed up the ocean
26 models. These operator interfaces are designed using native Fortran programming
27 language to smooth the learning curve.automatic parallelization. We further implement
28 a highly readable and efficient ocean model that contains only 1860 lines of code but
29 achieves a 91% parallel efficiency in strong scaling and 99% parallel efficiency in weak

30 scaling with 4096 Intel CPU cores. This ocean model also exhibits excellent scalability
31 on the heterogeneous Sunway TaihuLight supercomputer. This work presents a
32 promising alternative tool~~valuable example~~ for the development ~~of the next generation~~
33 of ocean models.

34

35 **Keywords:** implicit parallelism~~automatic parallelization~~, operator, ocean modelling,
36 parallel computing

37 1. Introduction

38 ~~Many earth system~~~~Numerous climate~~ models have been developed in the past several
39 decades to improve the predictive understanding of the ~~earth~~~~climate~~ system (Bonan and
40 Doney, 2018; Collins et al., 2018; Taylor et al., 2012). These models are becoming
41 increasingly complicated, and the amount of code has expanded from a few thousand
42 lines to tens of thousands ~~of lines~~, or even millions of lines. In terms of software
43 engineering, an increase in code causes the models to be more difficult to develop and
44 maintain.

45

46 The complexity of these models mainly originates from three aspects. ~~First, more model~~
47 ~~components and physical processes have been embedded into the earth system models,~~
48 ~~leading to a tenfold increase in the amount of code (e.g., Alexander and Easterbrook,~~
49 ~~2015). Second, some heterogeneous and advanced computing platforms (e.g.,~~
50 ~~Lawrence et al., 2018) have been widely used by the climate modelling community,~~
51 ~~resulting in a fivefold increase in the amount of code (e.g., Xu et al., 2015). Last, most~~
52 ~~of the model programs need~~~~First, more model components and physical processes have~~
53 ~~been embedded into the climate model, leading to a tenfold increase in the amount of~~
54 ~~code (Alexander and Easterbrook, 2015). Second, some heterogeneous and advanced~~
55 ~~computing platforms (Lawrence et al., 2018) have been widely applied by the climate~~
56 ~~community, resulting in a fivefold increase in the amount of code (Xu et al., 2015). Last,~~
57 ~~most of the model program needs~~ to be rewritten due to the continual development of
58 novel numerical methods and meshes. The promotion of novel numerical methods and
59 technologies produced in the fields of computational mathematics and computer
60 science have been limited in climate science because of the extremely heavy burden
61 caused by program rewriting and migration.

62

63 ~~Over the next few decades, tremendous computing capacities will be accompanied by~~
64 ~~more heterogeneous architectures which are equipped with two or more kinds of cores~~
65 ~~or processing elements (Shan, 2006), thus making for a much more sophisticated~~

66 computing environment for climate modellers than ever before (Bretherton et al., 2012).
67 Clearly, transiting the current earth system models to the next generation of computing
68 environments will be highly challenging and disruptive. Overall, complex codes in
69 earth system models combined with rapidly evolving computational techniques create
70 a very large gap between scientific aspiration and code implementation in the climate
71 modelling community.

72
73 ~~Over the next few decades, tremendous computing capacities will be accompanied by~~
74 ~~more heterogeneous architectures, thus making for a much more sophisticated~~
75 ~~computing environment for climate modellers than ever before (Bretherton et al., 2012).~~
76 ~~Clearly, transiting the current climate models to the next generation of computing~~
77 ~~environments will be highly challenging and disruptive. Overall, complex climate~~
78 ~~model codes combined with rapidly evolving computational techniques create a very~~
79 ~~large gap in climate science.~~

80
81 To reduce the complexity of earth system~~climate~~ models and bridge this gap, ~~we believe~~
82 ~~that~~ a universal and productive computing library is a promising~~probably the~~ solution.
83 Through establishing an implicit parallel and platform-independent computing library,
84 the complex models can be simplified and will no longer need explicit
85 parallelism~~parallelization~~ and transiting, thus effectively decoupling the development
86 of ocean models from complicated parallel computing techniques and diverse
87 heterogeneous computing platforms.

88
89 Many efforts have been made to address the complexity of parallel programming for
90 numerical simulations, such as operator overloading, source-to-source translator and
91 domain specific language (DSL). Operator overloading supports the customized data
92 type and provides simple operators and function interfaces to implement the model
93 algorithm. This technique is widely used because the implementation is straightforward
94 and easy to understand (Corliss and Griewank, 1994; Walther et al., 2003)~~Many studies~~

95 ~~have addressed the complexity of parallel programming for numerical simulations.~~
96 ~~Operator overloading is one of the mainstream implementations and is fairly~~
97 ~~straightforward (Corliss and Griewank, 1994; Walther et al., 2003). However, itthis~~
98 ~~method~~ is prone to work ~~inefficientlyinefficieney~~ because overloading execution
99 induces numerous unnecessary intermediate variables, consuming valuable memory
100 bandwidth resources. Using a source-to-source translator offers another solution. As
101 ~~indicated by the name,~~The important design philosophy of this method converts one
102 ~~language, which is usually strictly constrained by~~dependent on the simple self-defined
103 ~~rules, in the former language to another automatically generate code conforming to the~~
104 ~~latter language~~ (Bae et al., 2013; Lidman et al., 2012). It requires tremendous work to
105 develop and maintain a robust source-to-source compiler. Furthermore, DSLs can
106 provide high-level abstraction interfaces that use mathematical notations similar to
107 those used by domain scientists, so that they can write much more concise and more
108 straightforward code. Some outstanding DSLs,~~In the MIT General Circulation Model~~
109 ~~(MITgem), the modellers use OpenAD (Naumann et al., 2006; Utke et al., 2008), which~~
110 ~~is an automatic algorithmic differentiation tool with a set of mathematical and linguistic~~
111 ~~rules, to generate fairly efficient tangent linear and adjoint code (Aderoft et al., 2017).~~
112 ~~Moreover, some outstanding domain specific languages (DSL), such as ATMOL (van~~
113 ~~Engelen, 2001), ICON DSL (Torres et al., 2013), and STELLA (Gysi et al., 2015) and~~
114 ATLAS (Deconinck et al., 2017), are used by the numerical model community.
115 Although they seem source-to-source technique, DSLs are newly-defined languages
116 and produce executable programs instead of target languages. Therefore the new syntax
117 makes it difficult for the modellers to master the DSLs. In addition, most DSLs are not
118 yet supported by robust compilers due to their relatively short history. Most, provide
119 high-level abstraction interfaces that use mathematical notations similar to those used
120 by domain scientists so that they can write much more concise and simpler code.
121
122 ~~In fact, when using source to source translator and DSL methods to develop practical~~
123 ~~climate models, one major difficulty is the requirement of a stable and robust compiler,~~

124 ~~rather than an experimental compiler, at the product level. Another difficulty is that the~~
125 ~~climate modellers have to change their programming habits and master a new~~
126 ~~programming method through novel rules or DSLs instead of using Fortran, which they~~
127 ~~are most familiar with. The last difficulty is that although a small part of the existing~~
128 ~~source-to-source translators and DSLs currently support graphics processing units~~
129 ~~(GPUs), most~~ of the source-to-source translators and DSLs still do not support the
130 rapidly evolving heterogeneous computing platforms, ~~such as~~especially the Chinese
131 Sunway TaihuLight supercomputer which is based on the homegrown Sunway
132 heterogeneous many-core processors and located at the National Supercomputing
133 Center in Wuxi.

134
135 Other methods such as COARRAY Fortran and CPP templates provide alternative ways.
136 Using COARRAY Fortran, a modeller has to control the reading and writing operation
137 of each image (Mellor-Crummey et al., 2009). In a sense, one has to manipulate the
138 images in parallel instead of writing serial code. In term of CPP templates, it is usually
139 suitable for small code and difficult for debugging (Porkoláb et al., 2007).

140
141 Inspired by the philosophy of operator overloading, source-to-source translating and
142 DSLs, we integrated the advantages of these three methods into a simple computing
143 library which is called OpenArray. The main contributions of OpenArray are as follows:

- 144 • Easy-to-use. The modellers can write simple operator expressions in Fortran to
145 solve partial differential equations (PDEs). The entire program appears to be
146 serial and the modellers do not need to know any parallel computing techniques.
147 We summarized twelve basic generalized operators to support whole ~~model~~
148 calculations in a particular class of ocean models which use the finite
149 difference method and staggered grid ~~in OpenArray~~.
150 • High efficiency. We adopt some advanced ~~techniques~~methods, including
151 intermediate computation graphing, asynchronous communication, kernel
152 fusion, loop optimization, and vectorization, to decrease the consumption of

153 memory bandwidth and improve efficiency. Performance of the programs
154 implemented by OpenArray is similar to ~~the~~that of original ~~but~~parallel program
155 manually optimized ~~parallel program~~by experienced programmers.

156 • Portability. ~~Currently~~The current OpenArray ~~supports~~version support both CPU
157 and Sunway platforms. ~~More platforms including GPU will be supported in the~~
158 ~~future. The complexity~~The input of ~~cross-platform migration is moved from the~~
159 ~~models to~~ OpenArray. ~~The applications based on~~ ~~is a Fortran source file~~
160 ~~including the operator expression form; then, the intermediate C++ code is~~
161 ~~automatically generated by~~OpenArray ~~can then be migrated seamlessly to the~~
162 ~~supported. The final output is a program that is executable on different~~
163 ~~computing~~ platforms.

164

165 Furthermore, we developed a ~~numerical~~practical ocean model based on the Princeton
166 Ocean Model (POM, Blumberg and Mellor, 1987) to test the capability and efficiency
167 of OpenArray. The new model is called the Generalized Operator Model of the Ocean
168 (GOMO). Because the parallel computing details are completely hidden, GOMO
169 consists of only 1860 lines of Fortran code and is more easily understood and
170 maintained than the original POM. Moreover, GOMO exhibits excellent scalability and
171 portability ~~on both~~the central processing unit (CPU) and Sunway platforms.

172

173 The remainder of this paper is organized as follows. Section 2 introduces some concepts
174 and presents the detailed mathematical descriptions of formulating the PDEs into
175 operator expressions. Section 3 describes the detailed design and optimization
176 techniques of OpenArray. ~~The implementation~~Implementation of GOMO is described
177 in section 4. Section 5 evaluates the ~~performances~~performance of OpenArray and
178 GOMO. Finally, ~~discussion and conclusion~~oneclusions are given in section 6 ~~and 7,~~
179 ~~respectively.~~

180

181 2. Concepts of the Array, Operator, and Abstract Staggered Grid

182 In this section, we introduce three important concepts in OpenArray: Array, Operator
183 and Abstract Staggered Grid to illustrate the design of OpenArray.

184

185 2.1 Array

186 To achieve this simplicity, we designed a derived data type, *Array*, which inspired our
187 project name, OpenArray. The new *Array* data type comprises a series of information,
188 including a 3-dimensional (3D) array to store data, a pointer to the computational grid,
189 a Message Passing Interface (MPI) communicator, the size of the halo region and other
190 information about the data distribution. All the information is used to manipulate the
191 ~~Array~~ 3-dimensional array as ~~ana-complete~~ object to simplify the parallel computing. In
192 ~~the~~ traditional ocean models, calculations for each grid point and the i , j , and k loops in
193 the horizontal and vertical directions are unavoidable. The advantage of taking the
194 ~~Array~~ arrays as ~~ana-complete~~ object is the significant reduction in the number of loop
195 operations in the models, making the code more intuitive and readable. When using ~~the~~
196 OpenArray library in a program, one can use `type(Array)` to declare new variables.

197 2.2 Operator

198 To illustrate the concept of an operator, we first take a 2-dimensional (2D) continuous
199 equation solving sea surface elevation as an example:

$$200 \quad \frac{\partial \eta}{\partial t} + \frac{\partial DU}{\partial x} + \frac{\partial DV}{\partial y} = 0, \quad (1)$$

201 where η is the surface elevation, U and V are the zonal and meridional velocities, and
202 D is the depth of the fluid column. We choose the finite difference method and staggered
203 Arakawa C grid scheme, which are adopted by most regional ocean models. In Arakawa
204 C grid, D is calculated at the centers, U component is calculated at the left and right
205 side of the variable D , V component is calculated at the lower and upper side of the
206 variable D (Fig. 1). Variables (D , U , V) located at different positions own different sets
207 of grid increments. Taking the term $\frac{\partial DU}{\partial x}$ as an example, we firstly apply linear
208 interpolation to obtain the D 's value at U point represented by $tmpD$. Through a

209 backward difference to the product of $tmpD$ and U , then the discrete expression of $\frac{\partial DU}{\partial x}$
 210 can be obtained.

$$211 \quad \underline{tmpD(i+1,j) = 0.5*(D(i+1,j)+D(i,j))*U(i+1,j),} \quad (2)$$

212 and

$$213 \quad \underline{\frac{\partial DU}{\partial x} = \frac{tmpD(i+1,j)-tmpD(i,j)}{dx(i,j)^*} = \frac{0.5*(D(i+1,j)+D(i,j))*U(i+1,j)-0.5*(D(i,j)+D(i-1,j))*U(i,j)}{dx(i,j)^*},} \quad (3)$$

214 where $dx(i,j)^* = 0.5*(dx(i,j) + dx(i-1,j))$.

215
 216 In this way~~Then~~, the above continuous equation can be discretized into the following
 217 form.

$$218 \quad \underline{\frac{\eta_{t+1}(i,j)-\eta_{t-1}(i,j)}{2*dt} + \frac{0.5*(D(i+1,j)+D(i,j))*U(i+1,j)-0.5*(D(i,j)+D(i-1,j))*U(i,j)}{dx(i,j)^*} +} \\
 219 \quad \underline{\frac{0.5*(D(i,j+1)+D(i,j))*V(i,j+1)-0.5*(D(i,j)+D(i,j-1))*V(i,j)}{dy(i,j)^*} = 0,} \\
 220 \quad (4) \quad \underline{\frac{(D(i+1,j)+D(i,j))*U(i+1,j)-(D(i,j)+D(i-1,j))*U(i,j)}{dx(i,j)^*} +} \\
 221 \quad \underline{\frac{(D(i,j+1)+D(i,j))*V(i,j+1)-(D(i,j)+D(i,j-1))*V(i,j)}{dy(i,j)^*} = 0} \quad (2)$$

222 where $dx(i,j)^* = 0.5*(dx(i,j) + dx(i-1,j))$, $dy(i,j)^* = 0.5*(dy(i,j) + dy(i,j-1))$,~~where~~
 223 subscripts η_{t+1} and η_{t-1} denote the surface elevations at the $(t+1)$ time step and $(t-1)$ time
 224 step. To simplify the discrete form, we introduce some notation for the differentiation
 225 (δ_f^x, δ_b^y) and interpolation $(\bar{\bar{}}_f^x, \bar{\bar{}}_b^y)$. The δ and overbar symbols define the
 226 differential operator and average operator. The subscript x or y denotes that the
 227 operation acts in the x or y direction, and the superscript f or b denotes that the
 228 approximation operation is forward or backward.

229
 230 Table 1 lists the detailed definitions of the twelve basic operators. The term *var* denotes
 231 a ~~3D3-dimentional~~ model variable. All twelve operators for the finite difference
 232 calculations are named using three letters in the form [A|D][X|Y|Z][F|B]. The first letter
 233 contains two options, A or D, indicating an average or a differential operator. The
 234 second letter contains three options, X, Y or Z, representing the direction of the
 235 operation. The last letter contains two options, F or B, representing forward or
 236 backward operation. The dx , dy and dz are the distances between two adjacent grid
 237 points along the x , y and z directions.

238 Using the basic operators, Eq. (42) is expressed as:

$$239 \quad \frac{\eta_{t+1} - \eta_{t-1}}{2 * dt} + \delta_f^x (\bar{D}_b^x * U) + \delta_f^y (\bar{D}_b^y * V) = 0. \quad (5=0) \quad (3)$$

241 Thus,

$$242 \quad \eta_{t+1} = \eta_{t-1} - 2 * dt * (\delta_f^x (\bar{D}_b^x * U) + \delta_f^y (\bar{D}_b^y * V)). \quad (6) \quad (4)$$

244 Then, Eq. (64) can be easily translated into a line of code using operators (the bottom
245 left panel in Fig. 24). Compared with the pseudo-codes (the right panel), the
246 corresponding implementation by operators is more straightforward simpler and more
247 consistent with the equations.

248

249 Next, we will use the operators in shallow water equations, which are more complicated
250 than those in the previous case. Assuming that the flow is in hydrostatic balance and
251 that the density and viscosity coefficientseoefficient are constant, and neglecting the
252 molecular friction, the shallow water equations are:

$$253 \quad \frac{\partial \eta}{\partial t} + \frac{\partial DU}{\partial x} + \frac{\partial DV}{\partial y} = 0, \quad (7=0) \quad (5)$$

$$255 \quad \frac{\partial DU}{\partial t} + \frac{\partial DUU}{\partial x} + \frac{\partial DVU}{\partial y} - fVD = -gD \frac{\partial \eta}{\partial x} + \mu D \left(\frac{\partial^2 U}{\partial x^2} + \frac{\partial^2 U}{\partial y^2} \right), \quad (8) \quad (6)$$

$$257 \quad \frac{\partial DV}{\partial t} + \frac{\partial DUV}{\partial x} + \frac{\partial DVV}{\partial y} + fUD = -gD \frac{\partial \eta}{\partial y} + \mu D \left(\frac{\partial^2 V}{\partial x^2} + \frac{\partial^2 V}{\partial y^2} \right), \quad (9) \quad (7)$$

259 where f is the Coriolis parameter, g is the gravitational acceleration, and μ is the
260 coefficient of kinematic viscosity. Using the Arakawa C grid and leapfrog time
261 difference scheme, the discrete forms represented by operators are shown in Eq. (108)
262 ~ Eq. (124).

$$263 \quad \frac{\eta_{t+1} - \eta_{t-1}}{2 * dt} + \delta_f^x (\bar{D}_b^x * U) + \delta_f^y (\bar{D}_b^y * V) = 0.$$

264 ~~(10)~~ ~~(8)~~

265
$$\frac{D_{t+1}U_{t+1}-D_{t-1}U_{t-1}}{2*dt} + \delta_b^x(\overline{D_b^x} * U_f^x * \overline{U_f^x}) + \delta_f^y(\overline{D_b^y} * V_b^x * \overline{U_b^y}) - \overline{f \overline{V_f^y}} * D_b^x = -g *$$

266
$$\overline{D_b^x} * \delta_b^x(\eta) + \mu * \overline{D_b^x} * (\delta_f^x(U_{t-1}) + \delta_f^y(U_{t-1}))$$

267 ~~(11)~~ ~~(9)~~

268
$$\frac{D_{t+1}V_{t+1}-D_{t-1}V_{t-1}}{2*dt} + \delta_f^x(\overline{D_b^x} * U_b^y * \overline{V_b^x}) + \delta_b^y(\overline{D_b^y} * V_f^y * \overline{V_f^y}) + \overline{f \overline{U_f^x}} * D_b^y = -g *$$

269
$$\overline{D_b^y} * \delta_b^y(\eta) + \mu * \overline{D_b^y} * (\delta_f^x(V_{t-1}) + \delta_b^y(V_{t-1}))$$

270 ~~(12)~~ ~~(10)~~

271 As the shallow water equations are solved, spatial average and differential~~difference~~
 272 operations are called repeatedly. Implementing these~~Such~~ operations is troublesome
 273 and thuseonsume the vast majority of the computing resources when solving the
 274 shallow water equations. Therefore, it is favourable~~necessary~~ to abstract these common
 275 operations from PDEs and encapsulate them into user-friendly, platform-independent,
 276 and implicit parallel operators. As shown in Fig. 32, we require only 3 lines of code to
 277 solve the shallow water equations. This more realistic case suggests that even more
 278 complex PDEs can be constructed and solved by following this elegant approach.

279

280 2.3 Abstract staggered grid

281 Most ocean models are implemented based ~~on the basis of~~ the staggered Arakawa grids
 282 (Arakawa and Lamb, 1981; Griffies et al., 2000). The variables in ocean models are
 283 allocated at different grid points. The calculations that use these variables are performed
 284 after several reasonable interpolations or differences. When we call the differential
 285 operations on a staggered grid, the difference value between adjacent points should be
 286 divided by the grid increment to obtain the final result. Setting the correct grid
 287 increment for modellers is troublesome work that is extremely prone to error, especially
 288 when the grid is nonuniform. Therefore, we propose~~proposed~~ an abstract staggered grid
 289 to support flexible switching of operator calculations among different staggered grids.
 290 When the grid information is provided at the initialization phase of OpenArray, a set of
 291 grid increments, including horizontal increments (dx(i,j), dy(i,j)) and vertical increment

292 ($dz(k)$), will be combined with each corresponding physical variable through grid
293 binding. Thus, the operators can implicitly automatically set the correct grid increments
294 for different Array variables, even if the grid is nonuniform.

295
296 As shown in Fig. 43, the cubes in the (a), (b), (c), and (d) panels are the minimum
297 abstract grid accounting for 1/8 of the volume of ~~the~~ cube in ~~Panel~~the (e.)-panel. The
298 eight points of each cube are numbered sequentially from 0 to 7, and each point has a
299 set of grid increments, i.e., dx , dy and dz . For example, all the variables of an abstract
300 Arakawa A grid are located at Point 3. For the Arakawa B grid, the horizontal velocity
301 Array (U , V) ~~is~~are located at Point 0, the temperature (T), the salinity (S), and the depth
302 (D) are located at Point 3, and the vertical velocity Array (W) is located at Point 7. For
303 the Arakawa C grid, Array U is located at Point 2 and Array V is located at Point 1. In
304 contrast, for the Arakawa D grid, Array U is located at Point 1 and Array V is located
305 at Point 2.

306
307 When we call the average and differential operators mentioned in Table 1, for example,
308 on the abstract Arakawa C grid, the position of Array D is Point 3, and the average AXB
309 operator acting on Array D will change the position from Point 3 to Point 1. Since Array
310 U is also allocated at Point 1, the operation $AXB(D)*U$ is allowed. In addition, the
311 subsequent differential operator on Array $AXB(D)*U$ will change the position of Array
312 $DXF(AXB(D)*U)$ from Point 1 to Point 3.

313
314 The jumping rules of different operators are given in Table 2. Due to the design of the
315 abstract staggered grids, the jumping rules for the Arakawa A, B, C, and D grids are
316 fixed. A change in the position of an array is determined only by the direction of a
317 certain operator acting on that array.

318
319 If users change the Arakawa grid type, first the position information of each physical
320 variable need to be reset (Shown in Fig. 4). Then the discrete form of each equation

needs to be redesigned. We take the Eq. (1) switching from Arakawa C grid to Arakawa B grid as an example. The positions of the horizontal velocity Array U and Array V are changed to Point 0, Array η and Array D stay the same. The discrete form is changed from Eq. (4) to Eq. (13), the corresponding implementation by operators is changed from Eq. (6) to Eq. (14).

$$\frac{\eta_{t+1}(i,j) - \eta_{t-1}(i,j)}{2*dt} + \frac{0.25*(D(i+1,j)+D(i,j))*(U(i+1,j)+U(i+1,j+1)) - 0.25*(D(i,j)+D(i-1,j))*(U(i,j)+U(i,j+1))}{dx(i,j)} + \frac{0.25*(D(i,j+1)+D(i,j))*(V(i,j+1)+V(i+1,j+1)) - 0.25*(D(i,j)+D(i,j-1))*(V(i,j)+V(i+1,j))}{dy(i,j)} = 0, \quad (13)$$

$$\eta_{t+1} = \eta_{t-1} - 2 * dt * \left(\delta_f^x \left(\bar{D}_b^x * \bar{U}_f^y \right) + \delta_f^y \left(\bar{D}_b^y * \bar{V}_f^x \right) \right). \quad (14)$$

The position information and jumping rules ~~are can be~~ used to ~~implicitly automatically~~ check whether the discrete form of an equation is correct. The grid increments are hidden by all the differential operators, ~~thus it makesmaking~~ the code simple and clean. In addition, since the rules are suitable for multiple staggered Arakawa grids, the modellers can flexibly switch the ocean model between different Arakawa grids. Notably, the users of OpenArray should input the correct positions of each array in the initialization phase. The value of the position is an input parameter when declaring an Array. An error will be reported if an operation is performed between misplaced points.

Although most of the existing ocean models use finite difference or finite volume methods on structured or semi-structured meshes (e.g., Blumberg and Mellor, 1987; Shchepetkin and McWilliams, 2005), there are still some ocean models using unstructured meshes (e.g., Chen et al., 2003; Korn, 2017), and even the spectral element method (e.g., Levin et al., 2000). In our current work, we design the basic operators only for finite difference and finite volume methods with structured grids. More customized operators for the other numerical methods and meshes will be implemented in our future work.

3. Design of OpenArray

Through the above operator notations in Table 1, ocean modellers can quickly convert the discrete PDE equations into the corresponding operator expression forms. The main purpose of OpenArray is to make complex parallel programming transparent to the modellers. As illustrated in Fig. 5, although most of the existing ocean models use finite difference or finite volume methods on structured or semi-structured meshes, such as POM, the Modular Ocean Model (MOM) (Griffies, 2012), the Parallel Ocean Program (POP) (Smith et al., 2010), MITgcm (Aderoft et al., 2017), and the Regional Ocean Modeling System (ROMS) (Shechepetkin and McWilliams, 2005), there are still some ocean models using unstructured meshes, including Advanced Circulation model (ADCIRC) (Luettich et al., 1992), Finite Volume Coastal Ocean Model (FVCOM) (Chen et al., 2003), and Stanford Unstructured Nonhydrostatic Terrain-following Adaptive Navier Stokes Simulator (SUNTANS) (Fringer et al., 2006), and even the spectral element method (e.g. Levin et al., 2000). In our current work, we design the basic operator only for finite difference and finite volume methods with structured grids. More customized operator for the other numerical methods and meshes will be implemented in our future work.

3. Design of OpenArray

Through the above operator notations in Table 1, ocean modellers can quickly convert the discrete PDE equations into the corresponding operator expression forms. The main purpose of OpenArray is to make complex parallel programming transparent to the modellers. As illustrated in Fig. 4, we use a computation graph as an intermediate representation, meaning that the operator expression forms written in Fortran will be translated into a computation graph with a particular data structure. In addition, OpenArray will use the intermediate computation graph to analyse the dependency of the distributed data and automatically produce the underlying parallel code. Finally, we use stable and mature compilers, such as the GNU Compiler Collection (GCC), Intel compiler (ICC), and Sunway compiler (SWACC), to generate the executable

377 ~~programs~~~~program~~ according to different backend platforms. These four steps and some
378 related techniques are described in detail in this section.

379

380 **3.1 Operator expression**

381 Although the basic generalized operators listed in Table 1 are only suitable to execute
382 first-order difference, other high-order difference or even more complicated operations
383 can be combined by these basic operators. For example, a second-order difference
384 operation can be expressed as $\delta_f^x(\delta_b^x(var))$. Supposing the grid distance is uniform,
385 the corresponding discrete form is $[var(i+1,j,k)+var(i-1,j,k) -2* var(i,j,k)] / dx^2$. In
386 addition, the central difference operation can be expressed as $(\delta_f^x(var) + \delta_b^x(var))/2$
387 since the corresponding discrete form is $[var(i+1,j,k)-var(i-1,j,k)] / 2dx$.

388

389 Using these operators to express the discrete PDE equation, the code and formula are
390 very similar. We call this effect “the self-documenting code is the formula”. Fig. 65
391 shows the one-to-one correspondence of each item in the code and the items in the sea
392 surface elevation equation. The code is very easy to program and understand. Clearly,
393 the basic operators and the combined operators greatly simplify the development and
394 maintenance of ocean models. The complicated parallel and optimization techniques
395 ~~are hidden behind~~~~will be concealed by~~ these operators. Modellers no longer need to
396 care about details and can escape from the “parallelism swamp”, ~~and thus they~~ can
397 therefore concentrate on the scientific issues.

398

399 **3.2 Intermediate computation graph**

400 Considering the example mentioned in Fig. 65, if one needs to compute the term
401 $DXF(AXB(D)*u)$ with the traditional operator overloading method, one first computes
402 $AXB(D)$ and stores the result into a temporary array (named *tmp1*), and then executes
403 $(tmp1*u)$ and stores the result into a new array, *tmp2*. The last step is to compute
404 $DXF(tmp2)$ and store the result in a new array, *tmp3*. Numerous temporary arrays
405 consume a considerable amount of memory, making the efficiency of operator
406 overloading is poor.

407

408 To solve this problem, we convert an operator expression form into a directed and
409 acyclic graph, which consists of basic data and function nodes, to implement a so-called
410 lazy expression evaluation (Bloss et al., 1988; Reynolds, 1999). Unlike the traditional
411 operator overloading method, we overload all arithmetic functions to generate an
412 intermediate computation graph rather than to obtain the result of each function. This
413 method is widely used in deep learning frameworks, e.g., TensorFlow (Abadi et al.,
414 2016) and Theano (Bastien et al., 2012), to improve computing efficiency. Figure 76
415 shows the procedure of parsing the operator expression form of the sea level elevation
416 equation into a computation graph. The input variables in the square boxes include the
417 sea surface elevation (elb), the zonal velocity (u), the meridional velocity (v) and the
418 depth (D). $dt2$ is a constant equal to $2*dt$. The final output is the sea surface elevation
419 at the next time step (elf). The operators in the round boxes have been overloaded in
420 OpenArray. In summary, all the operators provided by OpenArray are functions for the
421 *Array* calculation, in which the “=” notation is the assignment function, the “-” notation
422 is the subtraction function, the “*” notation is the multiplication function, the “+”
423 notation is the addition function, DXF and DYF are the differential functions, and AXF
424 and AYF are the averageinterpolated functions.

425

426 **3.3 Code Automatic code generation**

427 Given a computation graph, we design a lightweight engine to automatically generate
428 the corresponding source code automatically (Fig. 87). Each operator node in the
429 computation graph is called a kernel. The sequence of all kernels in a graph is usually
430 fused into a large kernel function. Therefore, the underlying engine schedules and
431 executes the fused kernel once and obtains the final result directly without any auxiliary
432 or temporary variables. Simultaneously, the scheduling overhead of the computation
433 graph and the startup overhead of the basic kernels can be reduced.

434

435 Most of the scientific computational applications are limited by the memory bandwidth

436 and cannot fully exploit the computing power of a processor. Fortunately, kernel fusion
437 is an effective optimization method to improve memory locality. When two kernels
438 need to process some data, their fusion holds shared data in the memory. Prior to the
439 kernel fusion, the computation graph is ~~automatically~~ analysed to find the operator
440 nodes that can be fused, and the analysis results are stored in several subgraphs. Users
441 can access to any individual subgraph by assigning the subgraph to an intermediate
442 variable for diagnostic purposes. After being given a series of subgraphs, the underlying
443 engine dynamically generates the corresponding kernel function in C++ using just-in-
444 time (JIT) compilation techniques (Suganuma and Yasue, 2005). The JIT compiler used
445 in OpenArray can fuse numbers of operators into a large compiled kernel. The benefit
446 of fusing operators is to alleviate memory bandwidth limitations and improve
447 performance compared with executing operators one-by-one. In order to generate a
448 kernel function based on a subgraph, we first add the function header and variable
449 definitions according to the name and type in the *Array* structure. And then we add the
450 loop head through the dimension information. Finally, we perform a depth-first walk
451 on the expression tree to convert data, operators, and assignment nodes into a complete
452 expression including load variables, arithmetic operation, and equal symbol with C++
453 language.

454

455 Notably, the time to compile a single kernel function is short, but practical applications
456 usually need to be run for thousands of time steps, and the overhead of generating and
457 compiling the kernel functions for the computation graph is extremely high. Therefore,
458 we generate a fusion kernel function only once for each subgraph, and put it into a
459 function pool. Later, when facing the same computation subgraph, we fetch the
460 corresponding fusion kernel function directly from the pool.

461

462 Since the arrays in OpenArray are distributed among different processing units, and the
463 operator needs to use the data in the neighbouring points, in order to ensure the
464 correctness, it is necessary to check the data consistency before fusion. The use of

465 different data splitting methods for distributed arrays can greatly affect computing
466 performance. The current data splitting method in OpenArray is the widely used block-
467 based strategy. Solving PDEs on structured grids often divides the simulated domain
468 into blocks that are distributed to different processing units. However, the
469 ~~differential~~difference and average operators always require their neighbouring points to
470 perform array computations. Clearly, ocean modellers have to frequently call
471 corresponding functions to carefully control~~controlling~~ the communication of the local
472 boundary region ~~is tedious work for ocean modellers~~.

473

474 Therefore, we implemented a general boundary management module to
475 ~~implicitly~~automatically maintain and update the local boundary information so that the
476 modellers no longer need to address the message communication. The boundary
477 management module uses asynchronous communication to update and maintain the
478 data of the boundary region, which is useful for simultaneous computing and
479 communication. These procedures of asynchronous communication are implicitly
480 invoked when calling the basic kernel or the fused kernel to ensure that the parallel
481 details are completely transparent to the modellers. For the global boundary conditions
482 of the limited physical domains, the values at the physical border are always set to zero
483 within the operators and operator expressions. In realistic cases, the global boundary
484 conditions are set by a series of functions (e.g., radiation, wall) provided by OpenArray.

485

486 **3.4 Portable program for different backend platforms**

487 With the help of dynamic code generation and JIT compilation technology, OpenArray
488 can be ~~easily~~ migrated to different backend platforms. Several basic libraries, including
489 Boost C++ libraries and Armadillo library, are required. The JIT compilation module is
490 based on Low-Level-Virtual-Machine (LLVM), thus theoretically the module can only
491 be ported to platforms supporting LLVM. If LLVM is not supported, as on the Sunway
492 platform, one can generate the fusion kernels in advance by running the ocean model
493 on an X86 platform. If the target platform is CPUs with acceleration cards, such as GPU

494 clusters, it is necessary to add control statements in the CPU code, including data
495 transmission, calculation, synchronous and asynchronous statements. In addition, the
496 accelerating solution should involve the selection of the best parameters, for example
497 “blockDim” and “gridDim” on GPU platforms. In short, the code generation module of
498 OpenArray also needs to be refactored to be able to generate codes for different backend
499 platforms. The application based on OpenArray can then be migrated seamlessly to the
500 target platform. Currently, we have designed the corresponding source code generation
501 module for Intel CPU and Sunway processors in OpenArray.

502

503 According to the TOP500 list released in November 2018, the ~~The~~ Sunway TaihuLight
504 is ranked~~the~~ third-fastest supercomputer in the world, with a LINPACK benchmark
505 rating of 93 Petaflops provided by Sunway manya-multi-core processors (or Sunway
506 CPUs). As shown in Fig. 9, every Sunway CPU ~~Sunway processor that~~ includes 260
507 processing elements (or cores) that are divided into 4 core-groups. Each core-group,
508 ~~each of which~~ consists of 64 computing processing elements (CPEs) and a management
509 processing element (MPE) (Qiao et al., 2017). CPEs handle large-scale computing tasks
510 and MPE is responsible for the task scheduling and communication. The relationship
511 between MPE and CPE is like that between CPU and many-core accelerator, except for
512 they are fused into a single Sunway processor sharing a unified memory space. To make
513 the most of the computing resources of the Sunway TaihuLight, we generate kernel
514 functions for the MPE, which is responsible for the thread control, and CPE, which
515 performs the computations. The kernel functions are fully optimized with several code
516 optimization techniques (Pugh, 1991) such as loop tiling, loop aligning, single-
517 instruction multiple-date (SIMD) vectorization, and function inline. In addition, due to
518 the high memory access latency of CPEs, we accelerate data access by providing
519 instructions for direct memory access in the kernel to transfer data between the main
520 memory and local memory (Fu et al., 2017).

521

522 4. Implementation of GOMO

523 In this section, we introduce how to implement a ~~numericalpractical~~ ocean model using
524 OpenArray. The most important step is to derive the primitive discrete governing
525 equations in operator expression form, then the following work ~~iswill-be~~ completed
526 by OpenArray.

527

528 The fundamental equations of GOMO are derived from POM. GOMO features a
529 bottom-following, free-surface, staggered Arakawa C grid. To effectively evolve the
530 rapid surface fluctuations, GOMO uses the mode-splitting algorithm inherited from
531 POM to address the fast propagating surface gravity waves and slow propagating
532 internal waves in barotropic (external) and baroclinic (internal) modes, respectively.
533 The details of the continuous governing equations, the corresponding operator
534 expression form and the descriptions of all the variables used in GOMO are listed in
535 the Appendix A, Appendix B, and Appendix C, respectively.

536

537 Figure 108 shows the basic flow diagram of GOMO. At the beginning ~~of the workflow~~,
538 we initialize OpenArray to make all operators suitable for GOMO. After loading the
539 initial values and the model parameters, the distance information is input into the
540 differential operators through grid binding. In the external mode, the main consumption
541 is computing the ~~2D2-dimensional~~ sea surface elevation η and column-averaged
542 velocity (U_a , V_a). In the internal mode, ~~3D3-dimensional~~ array computations
543 predominate in order to calculate baroclinic motions (U , V , W), tracers (T , S , ρ), and
544 turbulence closure ~~schemesub-model~~ (q^2 , q^2l) (Mellor and Yamada, 1982), where (U , V ,
545 W) are the velocity fields in the x , y and σ directions, (T , S , ρ) are the potential
546 temperature, the salinity and the density. ($q^2/2$, $q^2l/2$) are the turbulence kinetic energy
547 and production of turbulence kinetic energy with turbulence length scale.

548

549 When the user dives into the GOMO code, the main time stepping loop in GOMO
550 appears to run on a single processor. However, as described above, implicit parallelism

551 is the most prominent feature of the program using OpenArray. The operators in
552 OpenArray, not only the difference and average operators, but also the “+”, “-”, “*”, “/”
553 and “=” operators in the Fortran code, are all overloaded for the special data structure
554 “Array”. The seemly serial Fortran code is implicitly converted to parallel C++ code
555 by OpenArray, and the parallelization is hidden from the modellers.

556
557 Because the complicated parallel optimization and tuning processes are decoupled from
558 the ocean modelling, we completely implemented GOMO based on OpenArray in only
559 4 weeks, whereas implementation may take several months or even longer when using
560 the MPI or CUDA library.

561
562 In comparison with the existing POM and its multiple variations, to name a few, Stony
563 Brook Parallel Ocean Model (sbPOM), mpiPOM and POMgpu, GOMO has less code
564 but is more powerful in terms of compatibility. As shown in Table 3, the serial version
565 of POM (POM2k) contains 3521 lines of code. sbPOM and mpiPOM are parallelized
566 using MPI, while POMgpu is based on MPI and CUDA-C. The codes of sbPOM,
567 mpiPOM and POMgpu are extended to 4801, 9680 and 30443 lines. In contrast, the
568 code of GOMO is decreased to 1860 lines. Moreover, GOMO completes the same
569 function as the other approaches while using the least amount of code (Table 4), since
570 the complexity has been transferred to OpenArray, which includes about 11,800 lines
571 of codes.:-

572
573 In addition, poor portability considerably restricts the use of advanced hardware in
574 oceanography. With the advantages of OpenArray, GOMO is adaptable to different
575 hardware architectures, such as the Sunway processor. The modellers do not need to
576 modify any code when changing platforms, ~~completely~~ eliminating the heavy burden
577 of transmitting code. As computing platforms become increasingly diverse and
578 complex, GOMO becomes more powerful and attractive than the machine-dependent
579 models.

580

581 **5. Results**

582 ~~5. Experimental results~~

583 In this section, we first evaluate the basic performance of OpenArray using benchmark
584 tests on a single CPU platform. After checking the correctness of GOMO through an
585 ideal seamount test case, we use GOMO to further test the scalability and efficiency of
586 OpenArray.

587

588 **5.1 Benchmark testing**

589 We choose ~~two~~~~four~~ typical PDEs and their implementations from Rodinia v3.1, which
590 is a benchmark suite for heterogeneous computing (Che et al., 2009), as the original
591 version. For comparison, we re-implement these ~~two~~~~four~~ PDEs using OpenArray. In
592 addition, we added two other test cases. As shown in Table 5, the 2D continuity equation
593 is used to solve sea surface height, and its continuous form is shown in Eq. (1). The 2D
594 heat diffusion equation is a parabolic PDE that describes the distribution of heat over
595 time in a given region. Hotspot is a thermal simulation used for estimating processor
596 temperature on structured grids (Che et al., 2009; Huang et al., 2006). We tested one
597 ~~2D2-dimensional~~ case (Hotspot2D) and one ~~3D3-dimensional~~ case (Hotspot3D) of this
598 program. The average runtime for 100 iterations is taken as the performance metric. All
599 tests are executed on a single workstation with an Intel Xeon E5-2650 CPU. The
600 experimental results show that the performance of OpenArray versions is comparable
601 to the original versions.

602

603 **5.2 Validation tests of GOMO**

604 The seamount problem proposed by Beckman and Haidvogel is a widely used ideal test
605 case for regional ocean models (Beckmann and Haidvogel, 1993). It is a stratified
606 Taylor column problem, which simulates the flow over an isolated seamount with a
607 constant salinity and a reference vertical temperature stratification. An eastward
608 horizontal current of 0.1 m/s is added at model initialization. The southern and northern

609 boundaries are closed. If the Rossby number is small, an obvious anticyclonic
610 circulation is trapped by the mount in the deep water.

611

612 Using the seamount test case, we compare GOMO and sbPOM results. The
613 configurations of both models are exactly the same. Figure 119 shows that GOMO and
614 sbPOM both capture the anticyclonic circulation at 3500 metres depth. The shaded plot
615 shows the surface elevation, and the array plot shows the current at 3500 metres. Figure
616 119(a), 119(b), and 119(c) are the results of GOMO, sbPOM, and the difference
617 (GOMO-sbPOM), respectively. The differences in the surface elevation and deep
618 currents between the two models are negligible (Fig. 119(c)).

619

620 5.3 The weak and strong scalability of GOMO

621 The seamount test case is used to compare the performance of sbPOM and GOMO in
622 a parallel environment. We use the X86 cluster at National Supercomputing Center in
623 Wuxi of China, which provides 5000 Intel Xeon E5-2650 v2 CPUs for our account at
624 most. Figure 12(a) shows the result of a strong scaling evaluation, in which
625 the model size is fixed at $2048 \times 2048 \times 50$. The dashed line indicates the ideal speedup.
626 For the largest parallelisms with 4096 processes, GOMO and sbPOM achieve 91% and
627 92% parallel efficiency, respectively. Figure 12(b) shows the weak scalability of
628 sbPOM and GOMO. In the weak scaling test, the model size for each process is fixed
629 at $128 \times 128 \times 50$, and the number of processes is gradually increased from 16 to 4096.
630 Taking the performance of 16 processes as a baseline, we determine that the parallel
631 efficiencies of GOMO and sbPOM using 4096 processes are 99.0% and 99.2%,
632 respectively.

633

634 5.4 Testing on the Sunway platform

635 We also test theThe strong scalability of GOMO is also tested on the Sunway
636 platform. TaihuLight supercomputer. Supposing that the baseline is the runtime of
637 GOMO at 10000 Sunway cores with a grid size of $4096 \times 4096 \times 50$, the parallel

638 efficiency of GOMO can still reach 85% at 150000 cores, as shown in Fig. [1344](#).
639 However, we notice that the scalability declines sharply when the number of cores
640 exceeds 150000. There are two reasons leading to this decline. First, the block size
641 assigned to each core decreases as the number of cores increases, causing more
642 communication during boundary region updating. Second, some processes cannot be
643 accelerated even though more computing resources are available; for example, the time
644 spent on creating the computation graph, generating the fusion kernels, and compiling
645 the JIT cannot be reduced. Even though the fusion-kernel codes are generated and
646 compiled only once at the beginning of a job, it consumes about 2 minutes. In a sense,
647 OpenArray performs better when processing large-scale data, and GOMO is more
648 suitable for high-resolution scenarios. In the future, we will further optimize the
649 communication and graph-creating modules to improve the efficiency for large-scale
650 cores.

651

652 ~~6. Conclusion~~ Discussion

653 As we mentioned in Section 1, the advantages of OpenArray are easy-to-use, high
654 efficiency and portability. Using OpenArray, the modellers without any parallel
655 computing skill and experience can write simple operator expressions in Fortran to
656 implement complex ocean models. The ocean models can be run on any CPU and
657 Sunway platforms which have deployed the OpenArray library. We call this effect
658 “write once, run everywhere”. Other similar libraries (e.g., ATMOL, ICON DSL, and
659 STELLA, COARRAY) require the users to manually control the boundary
660 communication and task scheduling to some extent. In contrast, OpenArray implements
661 completely implicit parallelism with user-friendly interfaces and programming
662 languages.

663

664 However, there are still several problems to be solved in the development of OpenArray.
665 The first issue is computational efficiency. Once a variable is in one of the processor
666 registers or in the highest speed cache, it should be used as much as possible before

667 being replaced. In fact, we should never to move variables more than once each
668 timestep. The memory consumption brought by overloading techniques is usually high
669 due to the unnecessary variable moving and unavoidable cache missing. The current
670 efficiency and scalability of GOMO are close to sbPOM, since we have adopted a series
671 of optimization methods, such as memory pool, graph computing, JIT compilation, and
672 vectorization, to alleviate the requirement of memory bandwidth. However, we have to
673 admit that we cannot fully solve the memory bandwidth limited problem at present. We
674 think that time skewing is a cache oblivious algorithm for stencil computations (Frigo
675 and Strumpfen, 2005), since it can exploit temporal locality optimally throughout the
676 entire memory hierarchy. In addition, the polyhedral model may be another potential
677 approach, which uses an abstract mathematical representation based on integer
678 polyhedral, to analyze and optimize the memory access pattern of a program.

679

680 The second issue is that the current OpenArray version cannot support customized
681 operators. When modellers try out another higher-order advection or any other
682 numerical scheme, the twelve basic operators provided by OpenArray are not abundant.
683 We consider using a template mechanism to support the customized operators. The
684 rules of operations are defined in a template file, where the calculation form of each
685 customized operator is described by a regular expression. If users want to add a
686 customized operator, they only need to append a regular expression into the template
687 file.

688

689 OpenArray and GOMO will continue to be developed, and the following three key
690 improvements are planned for the following years.

691

692 First, we are developing the GPU version of OpenArray. During the development, the
693 principle is to keep hot data staying in GPU memory or directly swapping between
694 GPUs and avoid returning data to the main CPU memory. NVLink provides high
695 bandwidth and outstanding scalability for GPU-to-CPU or GPU-to-GPU

696 communication, and addresses the interconnect issue for multi-GPU and multi-
697 GPU/CPU systems.

698
699 Second, the data Input/Output is becoming a bottleneck of earth system models as the
700 resolution increases rapidly. At present we encapsulate the PnetCDF library to provide
701 simple I/O interfaces, such as load operation and store operation. A climate fast
702 input/output (CFIO) library (Huang et al., 2014) will be implemented into OpenArray
703 in the next few years. The performance of CFIO is approximately 220% faster than
704 PnetCDF because of the overlapping of I/O and computing. CFIO will be merged into
705 the future version of OpenArray and the performance is expected to be further improved.

706
707 Finally, as most of the ocean models, GOMO also faces the load imbalance issue. We
708 are adding the more effective load balance schemes, including space-filling curve
709 (Dennis, 2007) and curvilinear orthogonal grids, into OpenArray in order to reduce the
710 computational cost on land points.

711
712 OpenArray is a product of collaboration between oceanographers and computer
713 scientists. It plays an important role to simplify the porting work on the Sunway
714 TaihuLight supercomputer. We believe that OpenArray and GOMO will continue to be
715 maintained and upgraded. We aim to promote it to the model community as a
716 development tool for future numerical models.

718 7. We designedConclusion

719 In this paper, we design a simple computing library (OpenArray) to decouple ocean
720 modelling and parallel computing. OpenArray provides twelve basic operators that are
721 abstracted from PDEs and extended to ocean model governing equations. These
722 operators feature user-friendly interfaces and an implicit parallelization ability.
723 FurthermoreMeanwhile, some state-of-art optimization mechanisms, including
724 computation graphing, kernel fusion, dynamic source code generation and JIT

725 compiling, are applied to boost the performance. The experimental results prove that
726 the performance of a program using OpenArray is comparable to that of well-designed
727 programs using Fortran. Based on OpenArray, we implement a numericalpractical
728 ocean model (GOMO) with ~~a~~-high productivity, ~~an~~-enhanced readability and ~~an~~
729 excellent scalable performance. Moreover, GOMO shows high scalability on both CPU
730 and the Sunway platform. Although more realistic tests are needed, OpenArray may
731 signal the beginning of a new frontier in future ocean modelling through ingesting basic
732 operators and cutting-edge computing techniques.

733

734 *Code availability.* The source codes of OpenArray v1.0 is available at
735 https://github.com/hxmhuang/OpenArray_CXX, and the user manual of OpenArray
736 can be accessed at https://github.com/hxmhuang/OpenArray_CXX/tree/master/doc.
737 GOMO is available at <https://github.com/hxmhuang/GOMO>.

738

739 **Appendix A: Continuous governing equations**

740 The equations governing the baroclinic (internal) mode in GOMO are the 3-
741 dimensional hydrostatic primitive equations.

$$742 \quad \frac{\partial \eta}{\partial t} + \frac{\partial UD}{\partial x} + \frac{\partial VD}{\partial y} + \frac{\partial W}{\partial \sigma} = 0, \quad (A1)$$

$$743 \quad \frac{\partial UD}{\partial t} + \frac{\partial U^2 D}{\partial x} + \frac{\partial UV D}{\partial y} + \frac{\partial UW}{\partial \sigma} - fVD + gD \frac{\partial \eta}{\partial x} = \frac{\partial}{\partial \sigma} \left(\frac{K_M}{D} \frac{\partial U}{\partial \sigma} \right) +$$

$$744 \quad \frac{gD^2}{\rho_0} \frac{\partial}{\partial x} \int_{\sigma}^0 \rho d\sigma' - \frac{gD}{\rho_0} \frac{\partial D}{\partial x} \int_{\sigma}^0 \sigma' \frac{\partial \rho}{\partial \sigma'} d\sigma' + F_{u, \sigma} \quad (A2)$$

$$745 \quad \frac{\partial VD}{\partial t} + \frac{\partial UV D}{\partial x} + \frac{\partial V^2 D}{\partial y} + \frac{\partial VW}{\partial \sigma} + fUD + gD \frac{\partial \eta}{\partial y} = \frac{\partial}{\partial \sigma} \left(\frac{K_M}{D} \frac{\partial V}{\partial \sigma} \right) +$$

$$746 \quad \frac{gD^2}{\rho_0} \frac{\partial}{\partial y} \int_{\sigma}^0 \rho d\sigma' - \frac{gD}{\rho_0} \frac{\partial D}{\partial y} \int_{\sigma}^0 \sigma' \frac{\partial \rho}{\partial \sigma'} d\sigma' + F_{v, \sigma} \quad (A3)$$

$$747 \quad \frac{\partial TD}{\partial t} + \frac{\partial TUD}{\partial x} + \frac{\partial TVD}{\partial y} + \frac{\partial TW}{\partial \sigma} = \frac{\partial}{\partial \sigma} \left(K_H \frac{\partial T}{\partial \sigma} \right) + F_T + \frac{\partial R}{\partial \sigma} \quad (A4)$$

$$748 \quad \frac{\partial SD}{\partial t} + \frac{\partial SUD}{\partial x} + \frac{\partial SV D}{\partial y} + \frac{\partial SW}{\partial \sigma} = \frac{\partial}{\partial \sigma} \left(K_H \frac{\partial S}{\partial \sigma} \right) + F_{S, \sigma} \quad (A5)$$

$$749 \quad \rho = \rho(T, S, p), \quad (A6)$$

$$750 \quad \frac{\partial q^2 D}{\partial t} + \frac{\partial Uq^2 D}{\partial x} + \frac{\partial Vq^2 D}{\partial y} + \frac{\partial Wq^2}{\partial \sigma} = \frac{\partial}{\partial \sigma} \left(\frac{K_q}{D} \frac{\partial q^2}{\partial \sigma} \right) + \frac{2K_M}{D} \left[\left(\frac{\partial U}{\partial \sigma} \right)^2 + \left(\frac{\partial V}{\partial \sigma} \right)^2 \right] +$$

$$751 \quad \frac{2g}{\rho_0} K_H \frac{\partial \rho}{\partial \sigma} - \frac{2Dq^3}{B_1 l} + F_{q^2} \quad (A7)$$

$$752 \quad \frac{\partial q^2 l D}{\partial t} + \frac{\partial U q^2 l D}{\partial x} + \frac{\partial V q^2 l D}{\partial y} + \frac{\partial W q^2 l}{\partial \sigma} = \frac{\partial}{\partial \sigma} \left(\frac{K_q}{D} \frac{\partial q^2 l}{\partial \sigma} \right) + E_1 l \left\{ \frac{K_M}{D} \left[\left(\frac{\partial U}{\partial \sigma} \right)^2 + \right. \right. \\ 753 \quad \left. \left. \left(\frac{\partial V}{\partial \sigma} \right)^2 \right] + \frac{g E_3}{\rho_0} K_H \frac{\partial \rho}{\partial \sigma} \right\} \tilde{W} - \frac{D q^3}{B_1} + F_{q^2 l} \quad (A8)$$

754

755 where ~~Where~~ F_u , F_v , F_{q^2} , and $F_{q^2 l}$ are horizontal kinematic viscosity terms of u , v , q^2 ,
756 and $q^2 l$, respectively. F_T and F_S are horizontal diffusion terms of T and S respectively.
757 \tilde{W} is the wall proximity function.

$$758 \quad F_u = \frac{\partial}{\partial x} (2A_M D \frac{\partial U}{\partial x}) + \frac{\partial}{\partial y} \left[A_M D \left(\frac{\partial U}{\partial y} + \frac{\partial V}{\partial x} \right) \right] \quad (A9)$$

$$759 \quad F_v = \frac{\partial}{\partial y} (2A_M D \frac{\partial V}{\partial y}) + \frac{\partial}{\partial x} \left[A_M D \left(\frac{\partial U}{\partial y} + \frac{\partial V}{\partial x} \right) \right] \quad (A10)$$

$$760 \quad F_T = \frac{\partial}{\partial x} (A_H H \frac{\partial T}{\partial x}) + \frac{\partial}{\partial y} (A_H H \frac{\partial T}{\partial y}) \quad (A11)$$

$$761 \quad F_S = \frac{\partial}{\partial x} (A_H H \frac{\partial S}{\partial x}) + \frac{\partial}{\partial y} (A_H H \frac{\partial S}{\partial y}) \quad (A12)$$

$$762 \quad F_{q^2} = \frac{\partial}{\partial x} (A_M H \frac{\partial q^2}{\partial x}) + \frac{\partial}{\partial y} (A_M H \frac{\partial q^2}{\partial y}) \quad (A13)$$

$$763 \quad F_{q^2 l} = \frac{\partial}{\partial x} (A_M H \frac{\partial q^2 l}{\partial x}) + \frac{\partial}{\partial y} (A_M H \frac{\partial q^2 l}{\partial y}) \quad (A14)$$

$$764 \quad \tilde{W} = 1 + \frac{E_2 l}{\kappa} \left(\frac{1}{\eta - z} + \frac{1}{H - z} \right) \quad (A15)$$

765 The equations governing the barotropic (external) mode in GOMO are obtained by
766 vertically integrating the baroclinic equations.

$$767 \quad \frac{\partial \eta}{\partial t} + \frac{\partial U_{AD}}{\partial x} + \frac{\partial V_{AD}}{\partial y} = 0 \quad (A16)$$

$$768 \quad \frac{\partial U_{AD}}{\partial t} + \frac{\partial (U_A)^2 D}{\partial x} + \frac{\partial U_A V_{AD}}{\partial y} - f V_{AD} + g D \frac{\partial \eta}{\partial x} = \tilde{F}_{u_a} - w u(0) + \\ 769 \quad w u(-1) - \frac{g D}{\rho_0} \int_{-1}^0 \int_{\sigma}^0 \left[D \frac{\partial \rho}{\partial x} - \frac{\partial D}{\partial x} \sigma' \frac{\partial \rho}{\partial \sigma} \right] d\sigma' d\sigma + G_{u_a} \quad (A17)$$

$$770 \quad \frac{\partial V_{AD}}{\partial t} + \frac{\partial U_A V_{AD}}{\partial y} + \frac{\partial (V_A)^2 D}{\partial y} + f U_{AD} + g D \frac{\partial \eta}{\partial y} = \tilde{F}_{v_a} - w v(0) + \\ 771 \quad w v(-1) - \frac{g D}{\rho_0} \int_{-1}^0 \int_{\sigma}^0 \left[D \frac{\partial \rho}{\partial y} - \frac{\partial D}{\partial y} \sigma' \frac{\partial \rho}{\partial \sigma} \right] d\sigma' d\sigma + G_{v_a} \quad (A18)$$

772

773 where ~~Where~~ \tilde{F}_{u_a} and \tilde{F}_{v_a} are the horizontal kinematic viscosity terms of U_A and V_A

774 respectively. G_{u_a} and G_{v_a} are the dispersion terms of U_A and V_A respectively. The
 775 subscript 'A' denotes vertical integration.

776

$$777 \quad \tilde{F}_{u_a} = \frac{\partial}{\partial x} \left[2H(AA_M) \frac{\partial U_A}{\partial x} \right] + \frac{\partial}{\partial y} \left[H(AA_M) \left(\frac{\partial U_A}{\partial y} + \frac{\partial V_A}{\partial x} \right) \right] \quad (A19)$$

$$778 \quad \tilde{F}_{v_a} = \frac{\partial}{\partial y} \left[2H(AA_M) \frac{\partial V_A}{\partial y} \right] + \frac{\partial}{\partial x} \left[H(AA_M) \left(\frac{\partial U_A}{\partial y} + \frac{\partial V_A}{\partial x} \right) \right] \quad (A20)$$

$$779 \quad G_{u_a} = \frac{\partial^2 (U_A)^2 D}{\partial x^2} + \frac{\partial^2 U_A V_A D}{\partial x \partial y} - \tilde{F}_{u_a} - \frac{\partial^2 (U^2)_{AD}}{\partial x^2} - \frac{\partial^2 (UV)_{AD}}{\partial y^2} + (F_u)_{A_z} \quad (A21)$$

$$780 \quad G_{v_a} = \frac{\partial^2 U_A V_A D}{\partial x \partial y} + \frac{\partial^2 (V_A)^2 D}{\partial y^2} - \tilde{F}_{v_a} - \frac{\partial^2 (UV)_{AD}}{\partial x^2} - \frac{\partial^2 (V^2)_{AD}}{\partial y^2} + (F_v)_{A_z} \quad (A22)$$

$$781 \quad U_A = \int_{-1}^0 U d\sigma_z \quad (A23)$$

$$782 \quad V_A = \int_{-1}^0 V d\sigma_z \quad (A24)$$

$$783 \quad (U^2)_A = \int_{-1}^0 U^2 d\sigma_z \quad (A25)$$

$$784 \quad (UV)_A = \int_{-1}^0 UV d\sigma_z \quad (A26)$$

$$785 \quad (V^2)_A = \int_{-1}^0 V^2 d\sigma_z \quad (A27)$$

$$786 \quad (F_u)_A = \int_{-1}^0 F_u d\sigma_z \quad (A28)$$

$$787 \quad (F_v)_A = \int_{-1}^0 F_v d\sigma_z \quad (A29)$$

$$788 \quad AA_M = \int_{-1}^0 (A_M) d\sigma_z \quad (A30)$$

789

790 **Appendix B: Discrete governing equations**

791 The discrete governing equations of baroclinic (internal) mode expressed by operators
 792 are shown as below:

$$793 \quad \frac{\eta^{t+1} - \eta^{t-1}}{2dti} + \delta_f^x (\overline{D}_b^x U) + \delta_f^y (\overline{D}_b^y V) + \delta_f^z (W) = 0_z \quad (B1)$$

$$794 \quad \frac{(\overline{D}_b^x U)^{t+1} - (\overline{D}_b^x U)^{t-1}}{2dti} + \delta_b^x \left[(\overline{D}_b^x U)_f \overline{U}_f^x \right] + \delta_f^y \left[(\overline{D}_b^y V)_b \overline{U}_b^y \right] +$$

$$795 \quad \delta_f^z (\overline{W}_b^x \overline{U}_b^z) - \overline{(\overline{V}_f^y D)}_b^x - \overline{(\overline{V}_f^y D)}_b^x + g \overline{D}_b^x \delta_b^x (\eta) = \delta_b^z \left[\frac{\overline{K}_{Mb}^x}{(\overline{D}_b^x)^{t+1}} \delta_f^z (U^{t+1}) \right] +$$

$$796 \quad \frac{g(\overline{D}_b^x)^2}{\rho_0} \int_{\sigma}^0 \left[\delta_b^x(\overline{\rho}_b^z) - \frac{\sigma}{\overline{D}_b^x} \delta_b^x(D) \delta_b^z(\overline{\rho}_b^x) \right] d\sigma' + F_{u_{\perp}} \quad (B2)$$

$$797 \quad \frac{(\overline{D}_b^y V)^{t+1} - (\overline{D}_b^y V)^{t-1}}{2dti} + \delta_f^x \left[\overline{(\overline{D}_b^x U)_b} \overline{V}_b^x \right] + \delta_b^y \left[\overline{(\overline{D}_b^y V)_f} \overline{V}_f^y \right] +$$

$$798 \quad \delta_f^z \left[\overline{W}_b^y \overline{V}_b^z \right] + \overline{(f \overline{U}_f^x D)_b}^y + \overline{(f \overline{U}_f^x D)_b}^y + g \overline{D}_b^y \delta_b^y(\eta) = \delta_b^z \left[\frac{\overline{K}_{M_b}^y}{(\overline{D}_b^y)^{t+1}} \delta_f^z(V^{t+1}) \right] +$$

$$799 \quad \frac{g(\overline{D}_b^y)^2}{\rho_0} \int_{\sigma}^0 \left[\delta_b^y(\overline{\rho}_b^z) - \frac{\sigma}{\overline{D}_b^y} \delta_b^y(D) \delta_b^z(\overline{\rho}_b^y) \right] d\sigma' + F_{v_{\perp}} \quad (B3)$$

$$800 \quad \frac{(\overline{TD})^{t+1} - (\overline{TD})^{t-1}}{2dti} + \delta_f^x(\overline{T}_b^x U \overline{D}_b^x) + \delta_f^y(\overline{T}_b^y V \overline{D}_b^y) + \delta_f^z(\overline{T}_b^z W) =$$

$$801 \quad \delta_b^z \left[\frac{\overline{K}_H}{\overline{D}^{t+1}} \delta_f^z(T^{t+1}) \right] + F_T + \delta_f^z R_{\perp} \quad (B4)$$

$$802 \quad \frac{(\overline{SD})^{t+1} - (\overline{SD})^{t-1}}{2dti} + \delta_f^x(\overline{S}_b^x U \overline{D}_b^x) + \delta_f^y(\overline{S}_b^y V \overline{D}_b^y) + \delta_f^z(\overline{S}_b^z W) =$$

$$803 \quad \delta_b^z \left[\frac{\overline{K}_H}{\overline{D}^{t+1}} \delta_f^z(S^{t+1}) \right] + F_{S_{\perp}} \quad (B5)$$

$$804 \quad \rho = \rho(T, S, p)_{\perp} \quad (B6)$$

$$805 \quad \frac{(\overline{q^2 D})^{t+1} - (\overline{q^2 D})^{t-1}}{2dti} + \delta_f^x(\overline{U}_b^z \overline{q^2}_b \overline{D}_b^x) + \delta_f^y(\overline{V}_b^z \overline{q^2}_b \overline{D}_b^y) +$$

$$806 \quad \delta_f^z(\overline{W q^2})_b^z = \delta_b^z \left[\frac{\overline{K}_{q_f}^z}{\overline{D}^{t+1}} \delta_f^z(q^2)^{t+1} \right] + \frac{2K_M}{D} \left\{ \left[\delta_b^z(\overline{U}_f^x) \right]^2 + \left[\delta_b^z(\overline{V}_f^y) \right]^2 \right\} +$$

$$807 \quad \frac{2g}{\rho_0} K_H \delta_b^z(\rho) - \frac{2Dq^3}{B_1 l} + F_{q^2_{\perp}} \quad (B7)$$

$$808 \quad \frac{(\overline{q^2 l D})^{t+1} - (\overline{q^2 l D})^{t-1}}{2dti} + \delta_f^x(\overline{U}_b^z \overline{q^2}_b \overline{l}_b \overline{D}_b^x) + \delta_f^y(\overline{V}_b^z \overline{q^2}_b \overline{l}_b \overline{D}_b^y) +$$

$$809 \quad \delta_f^z(\overline{W q^2 l})_b^z = \delta_b^z \left[\frac{\overline{K}_{q_f}^z}{\overline{D}^{t+1}} \delta_f^z(q^2 l)^{t+1} \right] + l E_1 \frac{K_M}{D} \left\{ \left[\delta_b^z(\overline{U}_f^x) \right]^2 + \left[\delta_b^z(\overline{V}_f^y) \right]^2 \right\} \tilde{W} +$$

$$810 \quad \frac{l E_1 E_3 g}{\rho_0} K_H \delta_b^z(\rho) \tilde{W} - \frac{Dq^3}{B_1} + F_{q^2 l_{\perp}} \quad (B8)$$

811

812 ~~where~~ **Where** F_u , F_v , F_{q^2} , and $F_{q^2 l}$ are horizontal kinematic viscosity terms of u , v , q^2 ,

813 and $q^2 l$, respectively. F_T and F_S are horizontal diffusion terms of T and S respectively.

$$814 \quad F_u = \delta_b^x \left[2A_M D \delta_f^x(U^{t-1}) \right] + \delta_f^x \left\{ \overline{(\overline{A}_{M_b}^x)_b}^y \overline{(\overline{D}_b^x)_b}^y \left[\delta_b^x(V)^{t-1} + \delta_b^y(U)^{t-1} \right] \right\}_{\perp} \quad (B9)$$

$$815 \quad F_v = \delta_b^y \left[2A_M D \delta_f^y(V^{t-1}) \right] + \delta_f^y \left\{ \overline{(\overline{A}_{M_b}^x)_b}^y \overline{(\overline{D}_b^x)_b}^y \left[\delta_b^x(V)^{t-1} + \delta_b^y(U)^{t-1} \right] \right\}_{\perp} \quad (B10)$$

$$816 \quad F_T = \delta_f^x \left[\overline{A_{H_b}^x} \overline{H_b^x} \delta_b^x (T^{t-1}) \right] + \delta_f^y \left[\overline{A_{H_b}^y} \overline{H_b^y} \delta_b^y (T^{t-1}) \right]. \quad (B11)$$

$$817 \quad F_S = \delta_f^x \left[\overline{A_{H_b}^x} \overline{H_b^x} \delta_b^x (S^{t-1}) \right] + \delta_f^y \left[\overline{A_{H_b}^y} \overline{H_b^y} \delta_b^y (S^{t-1}) \right]. \quad (B12)$$

$$818 \quad F_{q^2} = \delta_f^x \left[\overline{A_{M_b}^x} \overline{H_b^x} \delta_b^x (q^2)^{t-1} \right] + \delta_f^y \left[\overline{A_{M_b}^y} \overline{H_b^y} \delta_b^y (q^2)^{t-1} \right]. \quad (B13)$$

$$819 \quad F_{q^2 l} = \delta_f^x \left[\overline{A_{M_b}^x} \overline{H_b^x} \delta_b^x (q^2 l)^{t-1} \right] + \delta_f^y \left[\overline{A_{M_b}^y} \overline{H_b^y} \delta_b^y (q^2 l)^{t-1} \right]. \quad (B14)$$

820

821 The discrete governing equations of barotropic (external) mode expressed by operators
822 are shown as below:

$$823 \quad \frac{\eta^{t+1} - \eta^{t-1}}{2dte} + \delta_f^x (\overline{D_b^x} U_A) + \delta_f^y (\overline{D_b^y} V_A) = 0. \quad (B15)$$

$$824 \quad \frac{(\overline{D_b^x} U_A)^{t+1} - (\overline{D_b^x} U_A)^{t-1}}{2dte} + \delta_b^x \left[\overline{(\overline{D_b^x} U_A)_f} \overline{(U_A)_f^x} \right] + \delta_f^y \left[\overline{(\overline{D_b^y} V_A)_b} \overline{(U_A)_b^y} \right] -$$

$$825 \quad \left[\overline{\tilde{f}_A (V_A)_f^y D} \right]_b - \left[\overline{f (V_A)_f^y D} \right]_b + g \overline{D_b^x} \delta_b^x (\eta) = \delta_b^x \{ 2(AA_M) D \delta_f^x [(U_A)^{t-1}] \} +$$

$$826 \quad \delta_f^y \left\{ \left[\overline{(AA_M)_b^x} \right]_b \overline{(D_b^x)_b} [\delta_b^x (V_A) + \delta_b^y (U_A)]^{t-1} \right\} + \phi_x. \quad (B16)$$

$$827 \quad \frac{(\overline{D_b^y} V_A)^{t+1} - (\overline{D_b^y} V_A)^{t-1}}{2dte} + \delta_f^x \left[\overline{(\overline{D_b^x} U_A)_b} \overline{(V_A)_b^x} \right] + \delta_b^y \left[\overline{(\overline{D_b^y} V_A)_f} \overline{(V_A)_f^y} \right] +$$

$$828 \quad \left[\overline{\tilde{f}_A (U_A)_f^x D} \right]_b + \left[\overline{f (U_A)_f^x D} \right]_b + g \overline{D_b^y} \delta_b^y (\eta) = \delta_b^y \{ 2(AA_M) D \delta_f^y [(V_A)^{t-1}] \} +$$

$$829 \quad \delta_f^x \left\{ \left[\overline{(AA_M)_b^x} \right]_b \overline{(D_b^x)_b} [\delta_b^x (V_A) + \delta_b^y (U_A)]^{t-1} \right\} + \phi_y. \quad (B17)$$

830

831 where

$$832 \quad \phi_x = -WU(0) + WU(-1) - \frac{g(\overline{D_b^x})^2}{\rho_0} \int_{-1}^0 \left\{ \left[\int_{\sigma}^0 \delta_b^x (\overline{\rho})_b^z d\sigma' \right] d\sigma \right\} +$$

$$833 \quad \frac{g \overline{D_b^x} \delta_b^x D}{\rho_0} \int_{-1}^0 \left\{ \left[\int_{\sigma}^0 \overline{\sigma}_b^z \delta_b^z (\overline{\rho}_b^x) \right] d\sigma \right\} + G_x. \quad (B18)$$

$$834 \quad \phi_y = -WV(0) + WV(-1) - \frac{g(\overline{D_b^y})^2}{\rho_0} \int_{-1}^0 \left\{ \left[\int_{\sigma}^0 \delta_b^y (\overline{\rho})_b^z d\sigma' \right] d\sigma \right\} +$$

$$835 \quad \frac{g \overline{D_b^y} \delta_b^y D}{\rho_0} \int_{-1}^0 \left\{ \left[\int_{\sigma}^0 \overline{\sigma}_b^z \delta_b^z (\overline{\rho}_b^y) \right] d\sigma \right\} + G_y. \quad (B19)$$

836

837

838 **Appendix C: Descriptions of symbols**

839 The description of each symbol in the governing equations is list as below:

840 Table C1. Descriptions of symbols

Symbol	Description
η	Free surface elevation
H	Bottom topography
ua, va	Vertical average velocity in x, y direction, respectively
U, V, W	Velocity in x, y, σ direction, respectively
D	Fluid column depth
f	The Coriolis parameter
g	The gravitational acceleration
ρ_0	Constant density
ρ	Situ density
T	Potential temperature
S	Salinity
R	Surface solar radiation incident
$q^2/2$	Turbulence kinetic energy
l	Turbulence length scale
$q^2l/2$	Production of turbulence kinetic energy and turbulence length scale
dti	Time step of baroclinic mode
dte	Time step of barotropic mode
dx	Grid increment in x direction
dy	Grid increment in y direction
A_M	Horizontal kinematic viscosity
A_H	Horizontal heat diffusivity
K_M	Vertical kinematic viscosity
K_H	Vertical mixing coefficient of heat and salinity
K_q	Vertical mixing coefficient of turbulence kinetic energy

842 *Author contributions.* Xiaomeng Huang led the project of OpenArray and the writing
843 of this paper, Xing Huang, DW, QW, and SZ and Xing Huang designed OpenArray.
844 Xing Huang, DW, QW, SZ, MW, YG, and QT implemented and tested GOMO.
845 ~~All Xiaomeng Huang and Xing Huang led the writing of this paper with contributions~~
846 ~~from all other~~ coauthors contributed to the writing of this paper.

847

848 *Competing interests.* The authors declare that they have no conflict of interest.

849

850 *Acknowledgements.* Xiaomeng Huang is supported by a grant from the State's Key
851 Project of Research and Development Plan (2016YFB0201100) and the National
852 Natural Science Foundation of China (41776010). Xing Huang is supported by a grant
853 from the State's Key Project of Research and Development Plan (2018YFB0505000).
854 Shixun Zhang is supported by a grant from the State's Key Project of Research and
855 Development Plan (2017YFC1502200) and Qingdao National Laboratory for Marine
856 Science and Technology (QNL2016ORP0108). Zhenya Song is supported by
857 National Natural Science Foundation of China (U1806205) and AoShan Talents
858 Cultivation Excellent Scholar Program Supported by Qingdao National Laboratory for
859 Marine Science and Technology (2017ASTCP-ES04).

860

861 **References**

862 Abadi, M., Barham, P., Chen, J., Chen, Z., Davis, A., Dean, J., Devin, M., Ghemawat,
863 S., Irving, G., Isard, M., Kudlur, M., Levenberg, J., Monga, R., Moore, S., Murray,
864 D. G., Steiner, B., Tucker, P., Vasudevan, V., Warden, P., Wicke, M., Yu, Y. and
865 Zheng, X.: TensorFlow: A System for Large-Scale Machine Learning, in 12th
866 {USENIX} Symposium on Operating Systems Design and Implementation ({OSDI}
867 16), pp. 265–283, {USENIX} Association, Savannah, GA. [online] Available from:
868 <https://www.usenix.org/conference/osdi16/technical-sessions/presentation/abadi>,
869 2016.

870 ~~Aderoft, A., Campin, J. M., Dutkiewicz, S., Constantinos, E., Ferreira, D., Forget, G.,~~

871 ~~Fox-Kemper, B., Heimbach, P., Hill, C., Hill, E., Hill, H., Jahn, O., Losch, M.,~~
872 ~~Marshall, J., Maze, G., Menemenlis, D. and Molod, A.: MITgem User Manual,~~
873 ~~Intern. Doc., doi:1721.1/117188, 2017.~~

874 Alexander, K. and Easterbrook, S. M.: The software architecture of climate models: A
875 graphical comparison of CMIP5 and EMICAR5 configurations, *Geosci. Model Dev.*,
876 8(4), 1221–1232, doi:10.5194/gmd-8-1221-2015, 2015.

877 Arakawa, A. and Lamb, V. R.: A Potential Enstrophy and Energy Conserving Scheme
878 for the Shallow Water Equations, *Mon. Weather Rev.*, doi:10.1175/1520-
879 0493(1981)109<0018:APEAEC>2.0.CO;2, 1981.

880 Bae, H., Mustafa, D., Lee, J. W., Aurangzeb, Lin, H., Dave, C., Eigenmann, R. and
881 Midkiff, S. P.: The Cetus source-to-source compiler infrastructure: Overview and
882 evaluation, in *International Journal of Parallel Programming.*, 2013.

883 Bastien, F., Lamblin, P., Pascanu, R., Bergstra, J., Goodfellow, I. J., Bergeron, A.,
884 Bouchard, N., Warde-Farley, D. and Bengio, Y.: Theano: new features and speed
885 improvements, *CoRR*, abs/1211.5 [online] Available from:
886 <http://arxiv.org/abs/1211.5590>, 2012.

887 Beckmann, A. and Haidvogel, D. B.: Numerical simulation of flow around a tall
888 isolated seamount. Part I: problem formulation and model accuracy, *J. Phys.*
889 *Oceanogr.*, 23(8), 1736–1753, doi:10.1175/1520-
890 0485(1993)023<1736:NSOFAA>2.0.CO;2, 1993.

891 Bloss, A., Hudak, P. and Young, J.: Code optimizations for lazy evaluation, *Lisp Symb.*
892 *Comput.*, doi:10.1007/BF01806169, 1988.

893 Blumberg, A. F. and Mellor, G. L.: A description of a three-dimensional coastal ocean
894 circulation model, , (January 1987), 1–16, doi:10.1029/CO004p0001, 1987.

895 Bonan, G. B. and Doney, S. C.: Climate, ecosystems, and planetary futures: The
896 challenge to predict life in Earth system models, *Science* (80-.),
897 doi:10.1126/science.aam8328, 2018.

898 Bretherton, C., Balaji, V. ~~and~~, Delworth, T. et al: A National Strategy for Advancing
899 Climate Modeling, National Academies Press., 2012.

900 Che, S., Boyer, M., Meng, J., Tarjan, D., Sheaffer, J. W., Lee, S. H. and Skadron, K.:
901 Rodinia: A benchmark suite for heterogeneous computing, in Proceedings of the
902 2009 IEEE International Symposium on Workload Characterization, IISWC 2009.,
903 2009.

904 Chen, C., Liu, H. and Beardsley, R. C.: An unstructured grid, finite-volume, three-
905 dimensional, primitive equations ocean model: Application to coastal ocean and
906 estuaries, *J. Atmos. Ocean. Technol.*, doi:10.1175/1520-
907 0426(2003)020<0159:AUGFVT>2.0.CO;2, 2003.

908 Collins, M., Minobe, S., Barreiro, M., Bordoni, S., Kaspi, Y., Kuwano-Yoshida, A.,
909 Keenlyside, N., Manzini, E., O'Reilly, C. H., Sutton, R., Xie, S. P. and Zolina, O.:
910 Challenges and opportunities for improved understanding of regional climate
911 dynamics, *Nat. Clim. Chang.*, 8(2), 101–108, doi:10.1038/s41558-017-0059-8,
912 2018.

913 Corliss, G. and Griewank, A.: Operator Overloading as an Enabling Technology for
914 Automatic Differentiation, 1994.

915 [Deconinck, W., Bauer, P., Diamantakis, M., Hamrud, M., Kühnlein, C., Maciel, P.,](#)
916 [Mengaldo, G., Quintino, T., Raoult, B., Smolarkiewicz, P. K. and Wedi, N. P.: Atlas :](#)
917 [A library for numerical weather prediction and climate modelling, *Comput. Phys.*](#)
918 [Commun., 220, 188–204, doi:10.1016/j.cpc.2017.07.006, 2017.](#)

919 [Dennis, J. M.: Inverse space-filling curve partitioning of a global ocean model, *Proc. -*](#)
920 [21st Int. Parallel Distrib. Process. Symp. IPDPS 2007; Abstr. CD-ROM, 1–10,](#)
921 [doi:10.1109/IPDPS.2007.370215, 2007.](#)

922 van Engelen, R. a.: ATMOL: A Domain-Specific Language for Atmospheric Modeling,
923 *J. Comput. Inf. Technol.*, 9(4), 289–303, doi:10.2498/cit.2001.04.02, 2001.

924 [Frigo, M. and Strumpen, V.: Cache oblivious stencil computations, , 361,](#)
925 [doi:10.1145/1088149.1088197, 2005.](#)

926 ~~Fringer, O. B., Gerritsen, M. and Street, R. L.: An unstructured grid, finite volume,~~
927 ~~nonhydrostatic, parallel coastal ocean simulator, *Ocean Model.*,~~
928 ~~doi:10.1016/j.ocemod.2006.03.006, 2006.~~

929 Fu, H., He, C., Chen, B., Yin, Z., Zhang, Z., Zhang, W., Zhang, T., Xue, W., Liu, W.,
930 Yin, W. and others: 18.9-Pflops nonlinear earthquake simulation on Sunway
931 TaihuLight: enabling depiction of 18-Hz and 8-meter scenarios, in Proceedings of
932 the International Conference for High Performance Computing, Networking,
933 Storage and Analysis., 2017.

934 ~~Griffies, S. M.: Elements of the modular ocean model (MOM), GFDL Ocean Gr. Tech.~~
935 ~~Rep, 7(C), 620, 2012.~~

936 ~~Griffies, S. M.~~, Böning, C., Bryan, F. O., Chassignet, E. P., Gerdes, R., Hasumi, H.,
937 Hirst, A., Treguier, A.-M. and Webb, D.: Developments in ocean climate modelling,
938 Ocean Model., 2(3–4), 123–192, doi:10.1016/S1463-5003(00)00014-7, 2000.

939 Gysi, T., Osuna, C., Fuhrer, O., Bianco, M. and Schulthess, T. C.: STELLA: A Domain-
940 specific Tool for Structured Grid Methods in Weather and Climate Models, Proc.
941 Int. Conf. High Perform. Comput. Networking, Storage Anal. - SC '15, 1–12,
942 doi:10.1145/2807591.2807627, 2015.

943 Huang, W., Ghosh, S., Velusamy, S., Sankaranarayanan, K., Skadron, K. and Stan, M.
944 R.: HotSpot: A compact thermal modeling methodology for early-stage VLSI design,
945 IEEE Trans. Very Large Scale Integr. Syst., doi:10.1109/TVLSI.2006.876103, 2006.

946 Huang, X. M., Wang, W. C., Fu, H. H., Yang, G. W., Wang, B. and Zhang, C.: A fast
947 input/output library for high-resolution climate models, Geosci. Model Dev., 7(1),
948 93–103, doi:10.5194/gmd-7-93-2014, 2014.

949 Korn, P.: Formulation of an unstructured grid model for global ocean dynamics, J.
950 Comput. Phys., 339, 525–552, doi:10.1016/j.jcp.2017.03.009, 2017.

951 Lawrence, B. N., Rezny, M., Budich, R., Bauer, P., Behrens, J., Carter, M., Deconinck,
952 W., Ford, R., Maynard, C., Mullerworth, S., Osuna, C., Porter, A., Serradell, K.,
953 Valcke, S., Wedi, N. and Wilson, S.: Crossing the chasm: How to develop weather
954 and climate models for next generation computers?, Geosci. Model Dev.,
955 doi:10.5194/gmd-11-1799-2018, 2018.

956 Levin, J. G., Iskandarani, M. and Haidvogel, D. B.: A nonconforming spectral element
957 ocean model, Int. J. Numer. Methods Fluids, 34(6), 495–525, doi:10.1002/1097-

958 0363(20001130)34:6<495::AID-FLD68>3.0.CO;2-K, 2000.

959 Lidman, J., Quinlan, D. J., Liao, C. and McKee, S. A.: ROSE::FTTransform - A source-
960 to-source translation framework for exascale fault-tolerance research, Proc. Int.
961 Conf. Dependable Syst. Networks, (June), doi:10.1109/DSNW.2012.6264672, 2012.

962 ~~Mellor-Crummey, R. A., Westerink, J., Adhianto, L., Scherer III, W. N., J. and~~
963 ~~Jin, G.: A New Vision for Coarray Fortran, in Proceedings of the Third Conference~~
964 ~~on Partitioned Global Address Space Programming Models, p. 5:1--5:9, ACM, New~~
965 ~~York, NY, USA., 2009.~~

966 ~~Mellor, G. L.: Users guide for a~~~~Scheffner, N.: ADCIRC: an advanced~~ three-
967 dimensional, ~~primitive equation, numerical ocean circulation~~ model (June 2003
968 version), ~~Prog. Atmos. Ocean. Sci. Princet. Univ., (October), 53, 2003~~for shelves
969 coasts and estuaries, report 1: theory and methodology of ADCIRC-2DDI and
970 ADCIRC-3DL., 1992.

971 Mellor, G. L. and Yamada, T.: Development of a turbulence closure model for
972 geophysical fluid problems, Rev. Geophys., doi:10.1029/RG020i004p00851, 1982.

973 ~~Porkoláb, Z., Mihalicza, J. and Sipos, Á.: Debugging C++ template metaprograms, ,~~
974 ~~255, doi:10.1145/1173706.1173746, 2007.~~

975 ~~Naumann, U., Utke, J., Heimbach, P., Hill, C., Ozyurt, D., Wunsch, C., Fagan, M.,~~
976 ~~Tallent, N. and Strout, M.: Adjoint code by source transformation with OpenAD/F,~~
977 ~~Eur. Conf. Comput. Fluid Dyn. ECCOMAS CFD 2006, (September 2014), --, 2006.~~

978 Pugh, W.: Uniform Techniques for Loop Optimization, in Proceedings of the 5th
979 International Conference on Supercomputing, pp. 341–352, ACM, New York, NY,
980 USA., 1991.

981 Qiao, F., Zhao, W., Yin, X., Huang, X., Liu, X., Shu, Q., Wang, G., Song, Z., Li, X.,
982 Liu, H., Yang, G. and Yuan, Y.: A Highly Effective Global Surface Wave Numerical
983 Simulation with Ultra-High Resolution, in International Conference for High
984 Performance Computing, Networking, Storage and Analysis, SC., 2017.

985 Reynolds, J. C.: Theories of Programming Languages, Cambridge University Press,
986 New York, NY, USA., 1999.

987 Shan, A.: Heterogeneous Processing: A Strategy for Augmenting Moore's Law, Linux
988 J., 2006(142). Available from: <http://dl.acm.org/citation.cfm?id=1119128.1119135>,
989 2006.

990 Shchepetkin, A. F. and McWilliams, J. C.: The regional oceanic modeling system
991 (ROMS): A split-explicit, free-surface, topography-following-coordinate oceanic
992 model, Ocean Model., doi:10.1016/j.ocemod.2004.08.002, 2005.

993 ~~Smith, R., Jones, P., Briegleb, B., Bryan, F., Danabasoglu, G., Dennis, J., Dukowicz,~~
994 ~~J., Eden, C., Fox-Kemper, B., Gent, P., Hecht, M., Jayne, S., Jochem, M., Large,~~
995 ~~W., Lindsay, K., Maltrud, M., Norton, N., Peacock, S., Vertenstein, M. and Yeager,~~
996 ~~S.: The Parallel Ocean Program (POP) reference manual: Ocean component of the~~
997 ~~Community Climate System Model (CCSM), Los Alamos Natl. Lab. Tech. Rep.~~
998 ~~LAUR-10-01853, 141, 1–141 [online] Available from: www.cesm.ucar.edu/models~~
999 ~~/[cesm1.0/pop2/doc/sci/POPRefManual.pdf](http://www.cesm.ucar.edu/models/cesm1.0/pop2/doc/sci/POPRefManual.pdf), 2010.~~

1000 Suganuma, T. and Yasue, T.: Design and evaluation of dynamic optimizations for a
1001 Java just-in-time compiler, ACM Trans. ..., doi:10.1145/1075382.1075386, 2005.

1002 Taylor, K. E., Stouffer, R. J. and Meehl, G. A.: An overview of CMIP5 and the
1003 experiment design, Bull. Am. Meteorol. Soc., 93(4), 485–498, doi:10.1175/BAMS-
1004 D-11-00094.1, 2012.

1005 Torres, R., Linardakis, L., Kunkel, J. and Ludwig, T.: ICON DSL: A Domain-Specific
1006 Language for climate modeling, Sc13.Supercomputing.Org [online] Available from:
1007 <http://sc13.supercomputing.org/sites/default/files/WorkshopsArchive/pdfs/wp127s>
1008 1.pdf, 2013.

1009 ~~Utke, J., Naumann, U., Fagan, M., Tallent, N., Strout, M., Heimbach, P., Hill, C. and~~
1010 ~~Wunsch, C.: OpenAD/F: A Modular Open Source Tool for Automatic~~
1011 ~~Differentiation of Fortran Codes, ACM Trans. Math. Softw., 34(4), 18:1–18:36,~~
1012 ~~doi:10.1145/1377596.1377598, 2008.~~

1013 Walther, A., Griewank, A. and Vogel, O.: ADOL-C: Automatic Differentiation Using
1014 Operator Overloading in C++, PAMM, doi:10.1002/pamm.200310011, 2003.

1015 Xu, S., Huang, X., Oey, L. Y., Xu, F., Fu, H., Zhang, Y. and Yang, G.: POM.GPU-v1.0:

1016 A GPU-based princeton ocean model, Geosci. Model Dev., doi:10.5194/gmd-8-
1017 2815-2015, 2015.
1018
1019

Table 1. Definitions of the twelve basic operators

Notations	Discrete Form	Basic Operator
\overline{var}_f^x	$[var(i,j,k) + var(i+1,j,k)] / 2$	AXF
\overline{var}_b^x	$[var(i,j,k) + var(i-1,j,k)] / 2$	AXB
\overline{var}_f^y	$[var(i,j,k) + var(i,j+1,k)] / 2$	AYF
\overline{var}_b^y	$[var(i,j,k) + var(i,j-1,k)] / 2$	AYB
\overline{var}_f^z	$[var(i,j,k) + var(i,j,k+1)] / 2$	AZF
\overline{var}_b^z	$[var(i,j,k) + var(i,j,k-1)] / 2$	AZB
$\delta_f^x(var)$	$[var(i+1,j,k) - var(i,j,k)] / dx(i,j)$	DXF
$\delta_b^x(var)$	$[var(i,j,k) - var(i-1,j,k)] / dx(i-1,j)$	DXB
$\delta_f^y(var)$	$[var(i,j+1,k) - var(i,j,k)] / dy(i,j)$	DYF
$\delta_b^y(var)$	$[var(i,j,k) - var(i,j-1,k)] / dy(i,j-1)$	DYB
$\delta_f^z(var)$	$[var(i,j,k+1) - var(i,j,k)] / dz(k)$	DZF
$\delta_b^z(var)$	$[var(i,j,k) - var(i,j,k-1)] / dz(k-1)$	DZB

1024

Table 2 The jumping rules of an operator acting on an *Array*

The initial position of <i>var</i>	The position of $[A/D]X[F/B]$ (<i>var</i>)	The position of $[A/D]Y[F/B]$ (<i>var</i>)	The position of $[A/D]Z[F/B]$ (<i>var</i>)
0	1	2	4
1	0	3	5
2	3	0	6
3	2	1	7
4	5	6	0
5	4	7	1
6	7	4	2
7	6	5	3

1025

1026

1027

Table 3. Comparing GOMO with several variations of the POM

Model	Lines of code	Method	Computing Platforms
POM2k	3521	Serial	CPU
sbPOM	4801	MPI	CPU
mpiPOM	9685	MPI	CPU
POMgpu	30443	MPI + CUDA	GPU
GOMO	1860	OpenArray	CPU, Sunway

1028

1029

1030

Table. 4. Comparison of the amount of code for different functions

Functions	Lines of code		
	POM2k	sbPOM	GOMO
Solve for η	16	72	1
Solve for Ua	75	183	11
Solve for Va	75	183	11
Solve for W	36	90	3
Solve for q^2 and q^2l	318	854	162
Solve for T or S	178	234	71
Solve for U	118	230	50
Solve for V	118	230	50

1031

1032

1033

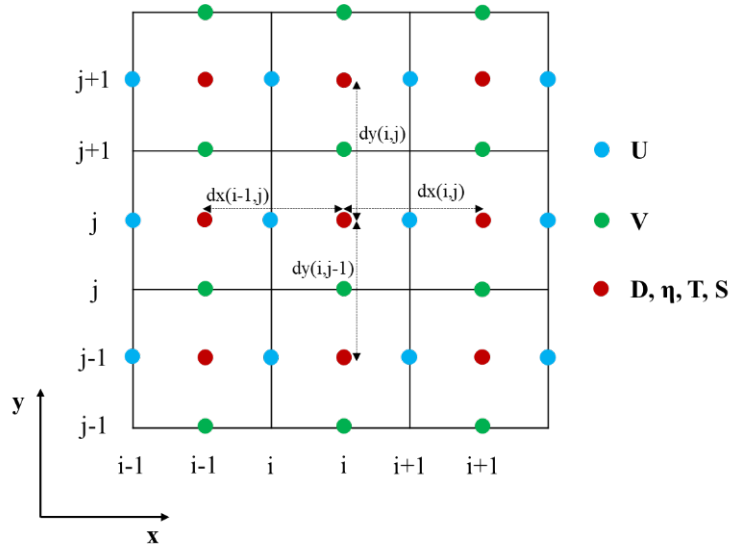
Table 5. Four benchmark tests

Benchmark	Dimensions	Grid Size	OpenArray version (seconds)	Original version(seconds)
Continuity equation	2D	8192×8192	7.22	7.10
Heat diffusion equation	2D	8192×8192	6.20	6.34
Hotspot2D	2D	8192×8192	11.37	11.21
Hotspot3D	3D	512×512×8	0.96	1.01

1034

1035

1037



1038

\$ 1) 2D continuous equation

$$\eta_{t+1} = \eta_{t-1} - 2 * dt * (\delta_x^2 (\bar{D}_b^x * U) + \delta_y^2 (\bar{D}_b^y * V))$$

\$ 3) The pseudo-code

```
exchange2d_mpi(u,im,jm)
exchange2d_mpi(v,im,jm)
exchange2d_mpi(D,im,jm)
```

\$ 2) The code constructed by operators

$$elf = elb - 2 * dt * (DXF(AXB(D)*U) + DYF(AYB(D)*V))$$

```
do i = 1, im
do j = 1, jm
elf(i,j) = elb(i,j) - 2 * dt * (
&
((D(i+1,j)+D(i,j))/2 * u(i+1,j) - (D(i,j)+D(i-1,j))/2 * u(i,j)) / dx(i,j) + &
((D(i,j+1)+D(i,j))/2 * v(i+1,j) - (D(i,j)+D(i,j-1))/2 * v(i,j)) / dy(i,j))
```

1039

1040

1041

Figure 1. Arrangement of variables in the staggered Arakawa C grid.

1042

\$ 1) 2D continuous equation

$$\eta_{t+1} = \eta_{t-1} - 2 * dt * (\delta_x^2 (\bar{D}_b^x * U) + \delta_y^2 (\bar{D}_b^y * V))$$

\$ 2) The code constructed by operators

$$elf = elb - 2 * dt * (DXF(AXB(D)*U) + DYF(AYB(D)*V))$$

\$ 3) The pseudo-code

```
exchange2d_mpi(u,im,jm)
exchange2d_mpi(v,im,jm)
exchange2d_mpi(D,im,jm)
```

```
do i = 1, im
```

```
do j = 1, jm
```

```
elf(i,j) = elb(i,j) - 2 * dt * (
    &
    ((D(i+1,j)+D(i,j))/2 * u(i+1,j) - (D(i,j)+D(i-1,j))/2 * u(i,j)) / dx(i,j) + &
    ((D(i,j+1)+D(i,j))/2 * v(i+1,j) - (D(i,j)+D(i,j-1))/2 * v(i,j)) / dy(i,j))
```

1043

1044

Figure 2. Implementation of Eq. (64) by basic operators. The *elf* and *elb* are the surface

1045

elevations at times $(t+1)$ and $(t-1)$ respectively.

1046

\$ Equation (8)

$$elf = elb - 2 * dt * (DXF(AXB(D) * U) + DYF(AYB(D) * V))$$

\$ Equation (9)

$$Uf = Db * Ub / Df - 2 * dt / Df * (DXB(AXF(AXB(D) * U) * AXF(U)) + DYF(AXB(AYB(D) * V) * AYB(U)) - & \\ AXB(f * AYF(V) * D) + g * AXB(D) * DXB(el) - aam * AXB(D) * (DXB(DXF(Ub)) + DYF(DYB(Ub)))))$$

\$ Equation (10)

$$Vf = Db * Vb / Df - 2 * dt / Df * (DXF(AYB(AXB(D) * U) * AXB(V)) + DYB(AYF(AYB(D) * V) * AYF(V)) + & \\ AYB(f * AXF(U) * D) + g * AYB(D) * DYB(el) - aam * AYB(D) * (DXF(DXB(Vb)) + DYB(DYF(Vb)))))$$

1047

1048

1049

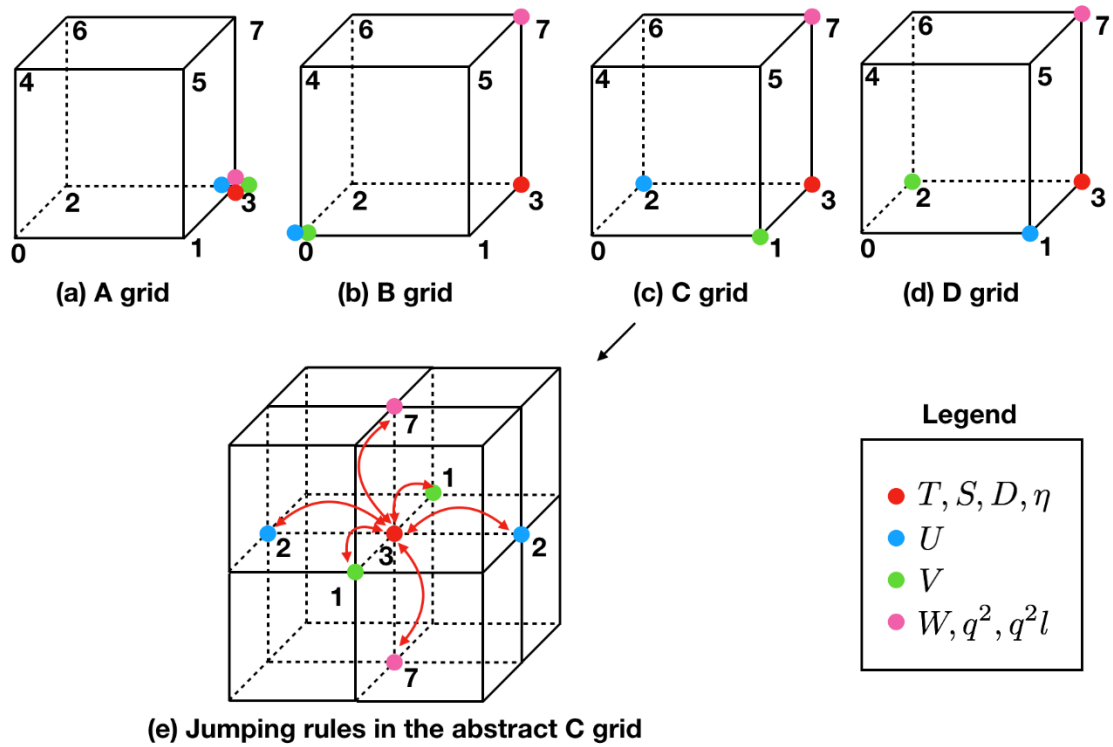
1050

1051

1052

1053

Figure 32. Implementation of the shallow water equations by basic operators. *elf*, *el* and *elb* denote sea surface elevations at times $(t+1)$, t and $(t-1)$, respectively. *Uf*, *U* and *Ub* denote the zonal velocity at times $(t+1)$, t and $(t-1)$, respectively. *Vf*, *V* and *Vb* denote the meridional velocity at times $(t+1)$, t and $(t-1)$, respectively. *aam* denotes the viscosity coefficient.



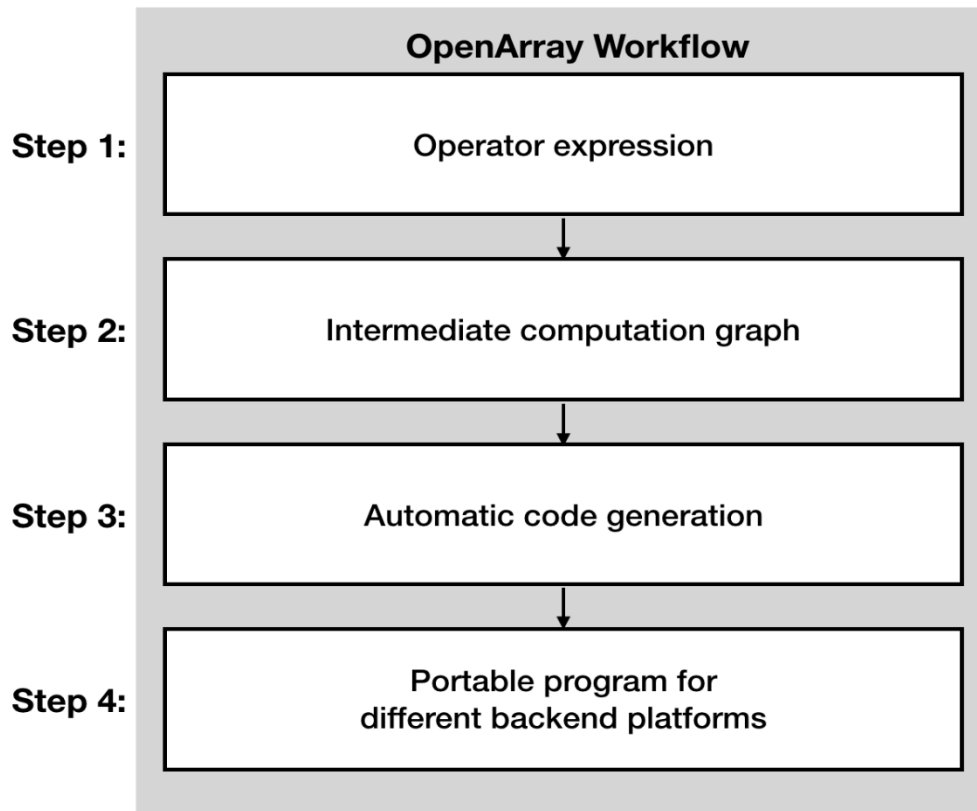
1054

1055

1056

1057

Figure 43. The schematic diagram of the relative positions of the variables on the abstract staggered grid and the jumping procedures among the grid points.



1058
|
1059
1060

Figure 54. The workflow of OpenArray.

Formula	$\eta_{t+1} = \eta_{t-1} - 2 * dt * \left(\delta_f^x (\bar{D}_b^x * U) + \delta_f^y (\bar{D}_b^y * V) \right)$
Code	$elf = elb - dt2 * (DXF(AXB(D)*U) + DYF(AYB(D)*V))$

1061

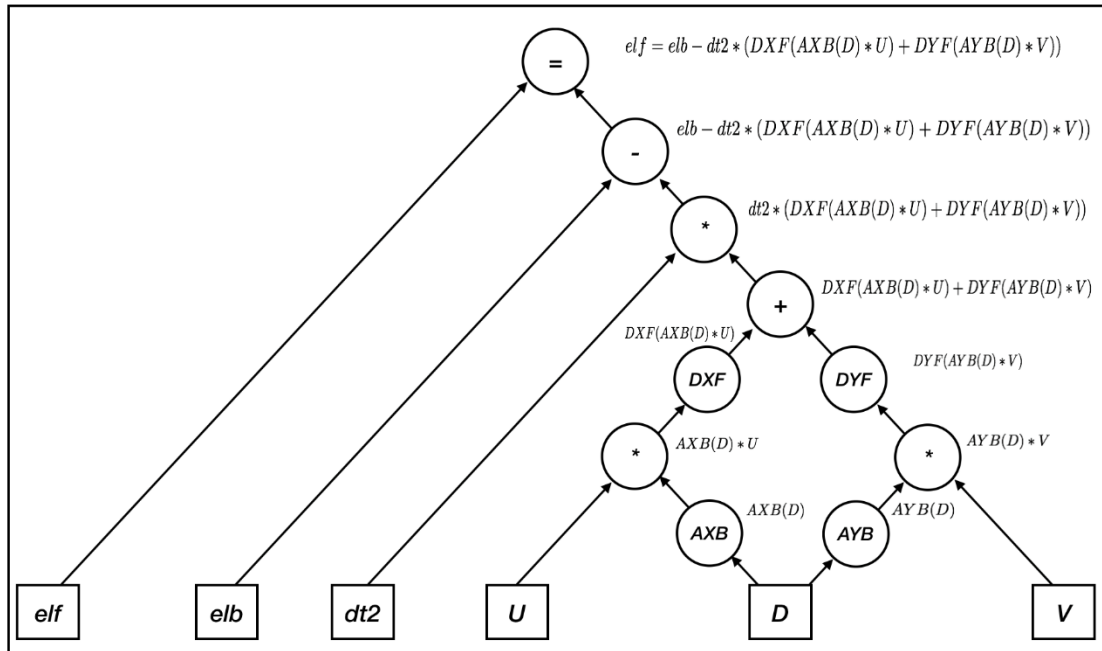
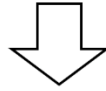
1062

1063

1064

Figure 65. The effect of “The self-documenting code is the formula” illustrated by the sea surface elevation equation.

$$elf = elb - dt2 * (DXF(AXB(D) * U) + DYF(AYB(D) * V))$$



1065
1066
1067

Figure 76. Parsing the operator expression form into the computation graph.

1068
1069
1070

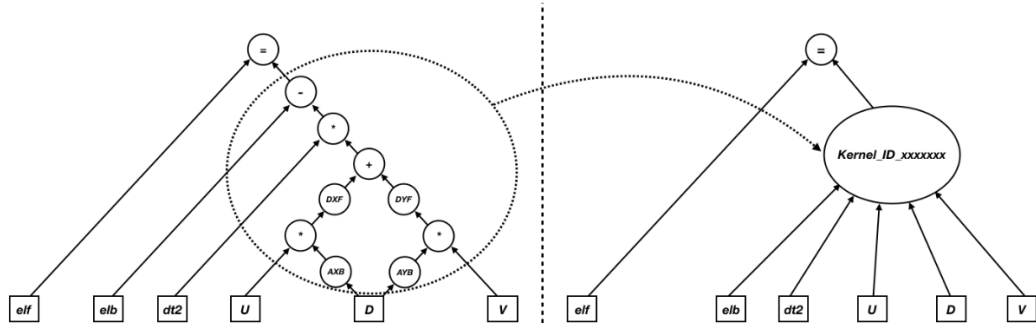
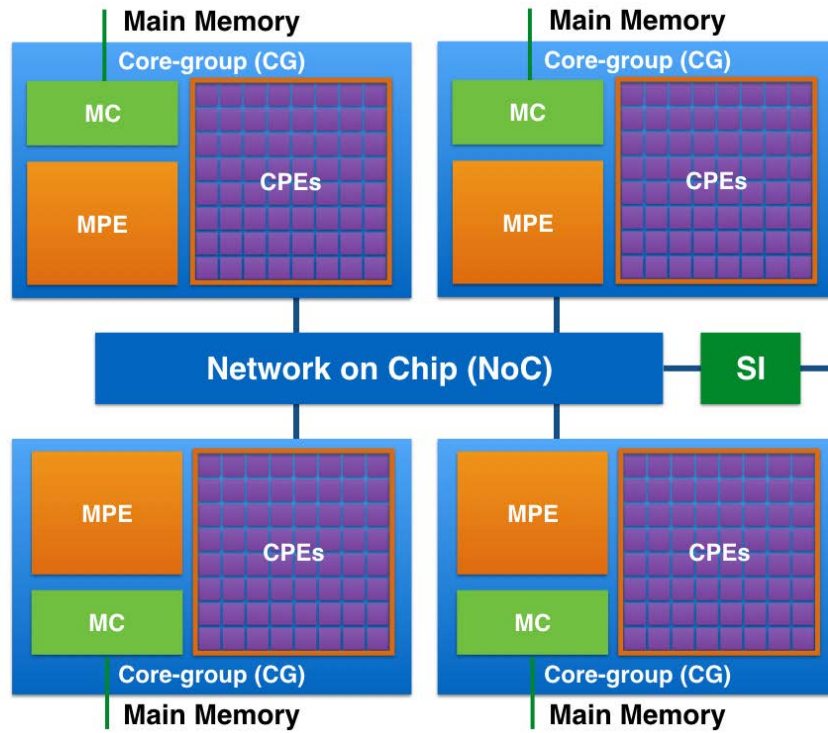


Figure 87. The schematic diagram of kernel fusion.

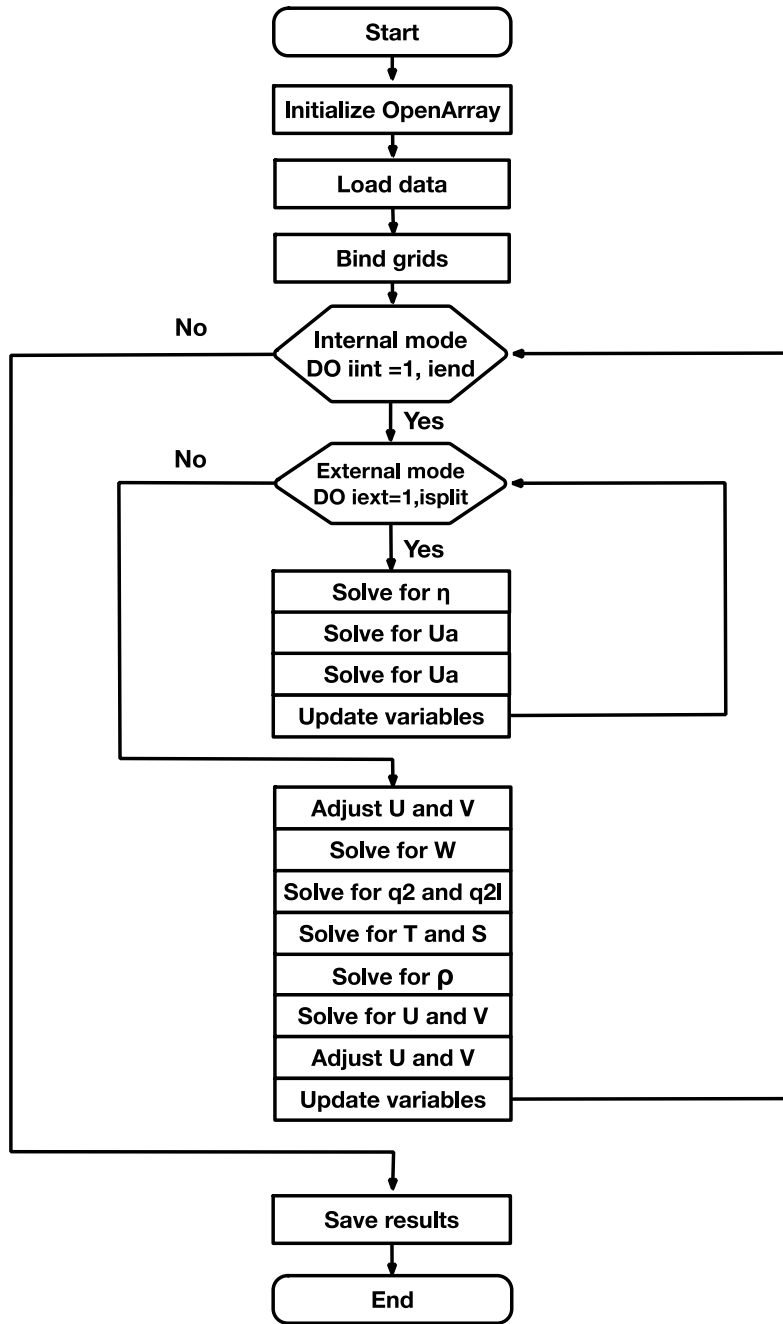
1071



1072

1073 Figure 9. The MPE-CPEs hybrid architecture of the Sunway processor. Every Sunway
1074 processor includes 4 Core-groups (CGs) connected by the Network on Chip (NoC).
1075 Each CG consists of a management processing element (MPE), 64 computing
1076 processing elements (CPEs) and a memory controller (MC). The Sunway processor
1077 uses the system interface (SI) to connect with outside devices.

1078



1079

1080

Figure 10.

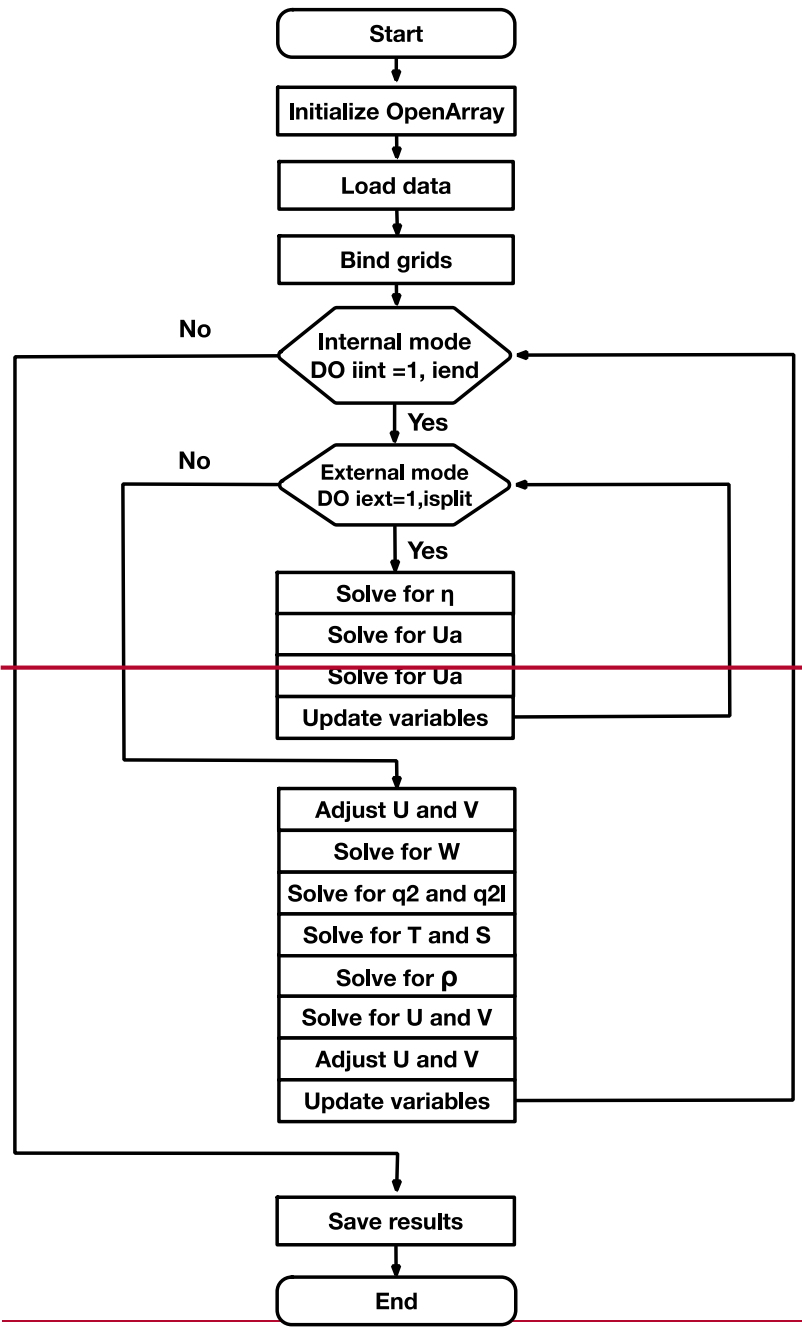
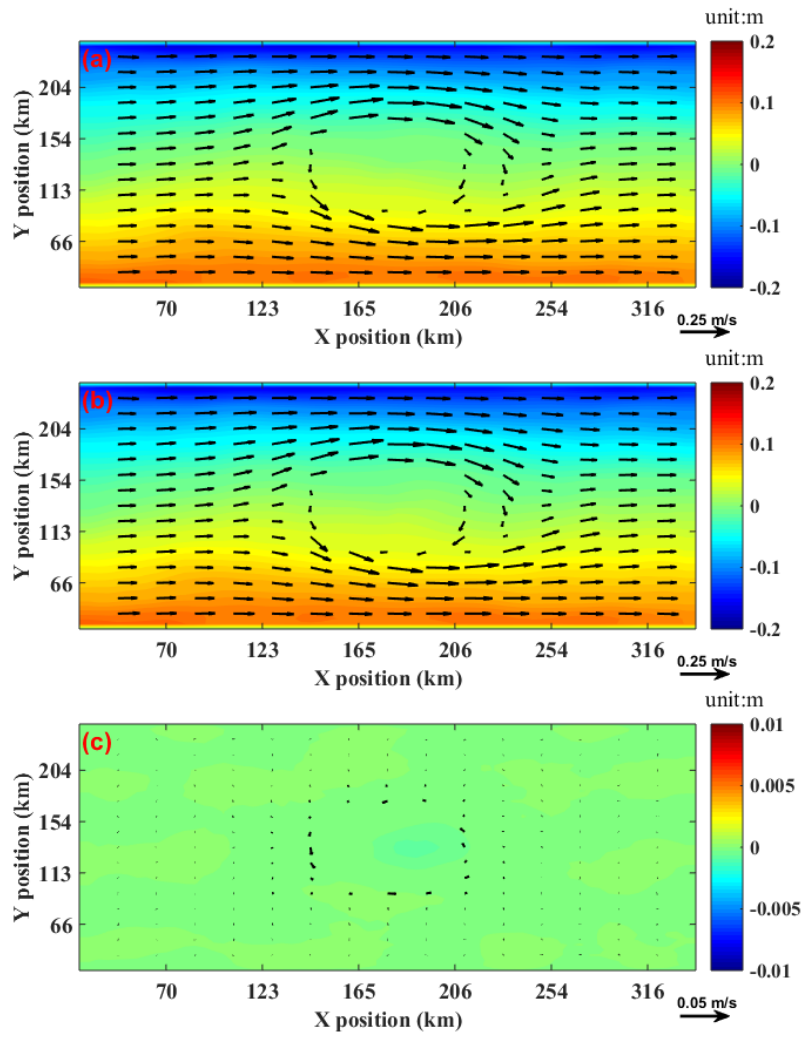


Figure 8. Flow diagram of GOMO

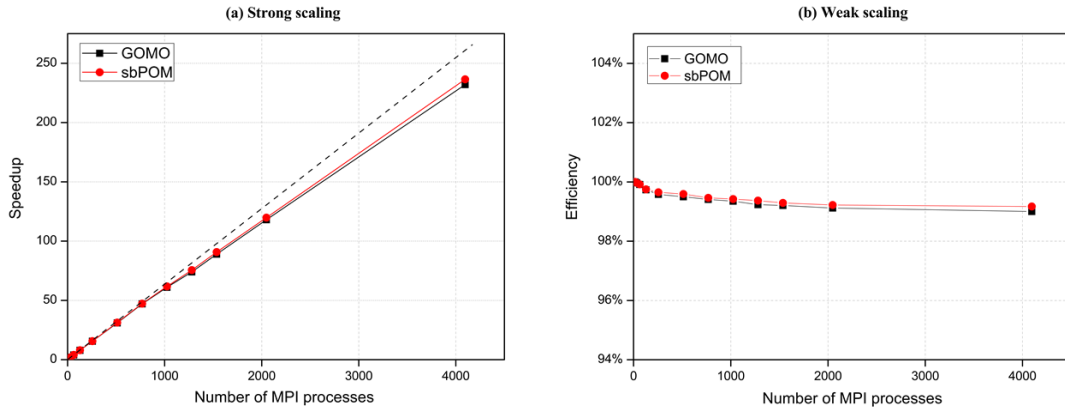
1081
1082
1083



1084

1085 Figure 119. Comparison of the surface elevation (shaded) and currents at 3500 metres
 1086 depth (vector) between GOMO and sbPOM on the 4th model day. (a) GOMO, (b)
 1087 sbPOM, (c) GOMO-sbPOM.

1088



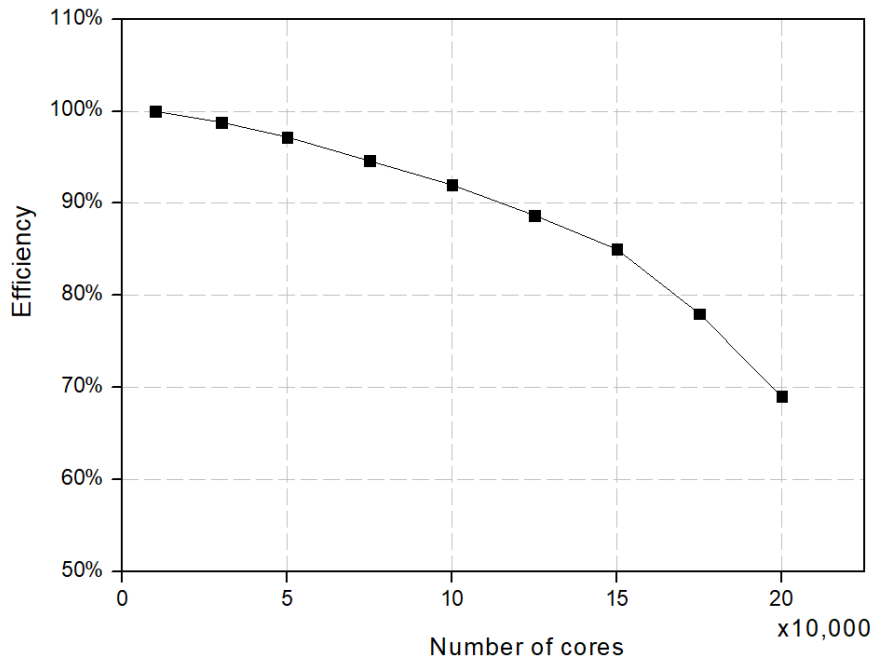
1089

1090 Figure 1240. Performance comparison between sbPOM and GOMO on the X86 cluster.

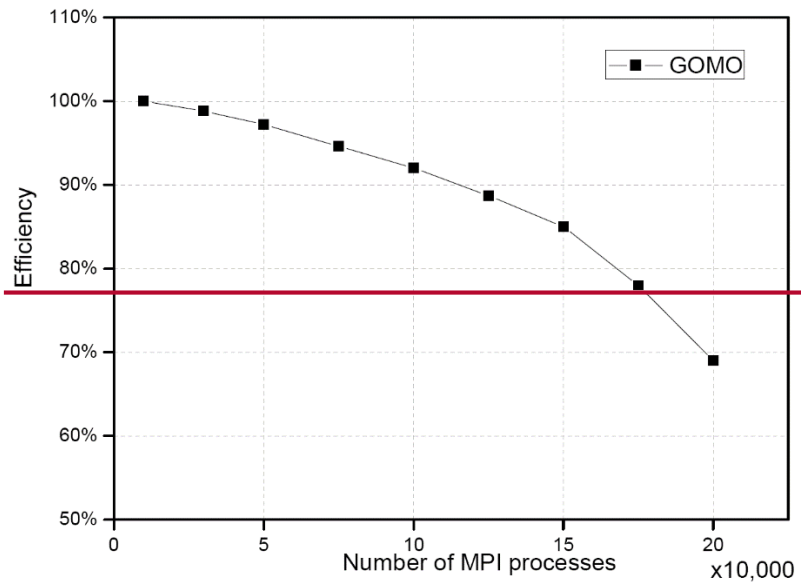
1091 (a) The strong scaling result; vertical axis denotes the speedup relative to 16 processes

1092 in a single node. (b) The weak scaling result.

1093



1094



1095

1096

Figure 1344. Parallel efficiency of GOMO on the Sunway platformTaihuLight superecomputer.

1097

1098